



ISAS - INTERNATIONAL SCHOOL FOR ADVANCED STUDIES

Academic year 1981-82

"POLYMORPHIC TRANSITION IN ALKALI HALIDES"

Thesis for the title of "Magister Philosophiae"

Candidate:

Chen Chuan-Hong

Supervisor:

Prof. M. PARRINELLO

27 October 1982

TRIESTE

POLYMORPHIC TRANSITION IN ALKALI HALIDES

Chen Chuan-hong

INTERNATIONAL SCHOOL FOR ADVANCED STUDIES IN TRIESTE

1982

POLYMORPHIC TRANSFORMATION IN ALKALI HALIDES

CONTENTS

I.	Introduction	(1)
II.	Some Geometrical Aspects of B1 and B2 Structures	(5)
III.	New Molecular Dynamics Method	(15)
IV.	A Static Study	(21)
	Concluding Remarks	(43)
	Acknowledgments	(44)
	References	(45)

I. Introduction

Prediction of the absolute and relative stability of different solid modification of a substance at atmospheric pressure, and the effects of varying external conditions on stability, is an important aspect of the theory of cohesion in solids. The theory of various structure phase transition in the solid state is really a difficult one, as the energy difference between different phases is in many cases a very small fraction of the total cohesive energy, of magnitude comparable with the accuracy of the cohesive energy itself. Alkali halides system is sufficiently simple and well studied class of solids [1]-[12] that may create favourable conditions for overcoming this difficulty. The rocksalt phase (as B1) to cesium chloride (B2) transformation in Alkali halides has been studied both experimentally and theoretically by a large number of investigators [13] since the discovery of this transition by Slater [14]. The transformation has been found to be a first order and reversible [15]. The transitions which have been most extensively studied are the structure changes of the chlorides, bromides and iodides of potassium and rubidium to the B2 structure at pressures of the order of 20 and 5Kb respectively [16], and of cesium chloride to B1 structure at 450°C [17]. The X-ray studies under pressure have revealed transitions to the B2 structure for the fluorides of potassium, rubidium and cesium [18] and for sodium chloride [19]. The neutron scattering has been used to elucidate the microscopic mechanism of the B1 to B2 transformation [20].

The first detailed theoretical studies of the B1 to B2 transformation were those of Jacobs [21]. A summary of the subject was given by Born and Huang [22]. A more detailed survey is to be found in the review by Tosi and Arai [23] and by Tosi and Fumi [24]. More recently, the spirit of various theoretical approaches has been reviewed by Gordon and Kim [25].

Cohen and Gordon [26] used the parameter free potential functions developed by Gordon and Kim [27], to study the B1 to B2 transition and this study was extended by Boyer [28] who included the effect of harmonic vibrations in the calculation of the free energy; this however did not materially

affect the conclusions based on static calculation.

The kinetics of polymorphic transition has not received much attention because of the intrinsic difficulty of the problem. Different microscopic mechanisms for the transformation from B1 to B2 structure have been postulated by many authors. As early as 1931 Shoji⁽²⁹⁾ had described a lattice deformation based on geometrical arguments, transforming the B1 to B2 structure. Buerger⁽³⁰⁾ illustrated this mechanism which consists of a compression along the $[1,1,1]$ direction and a dilation perpendicular to it. Later Fraser and Kennedy⁽³¹⁾ and Watanabe et.al⁽³²⁾ presented further deformation mechanisms. However, most of these theories are based only on the orientational relation observed during the transformation in some alkali halides and did not give a description of the microscopic origin of the proposed geometrical deformations. Recently, the encouraging progress has been made by Blaschko et.al. In their neutron scattering studies of the B1 to B2 transformation in RbI, Blaschko et.al.^{(20), (33)-(36)} investigated the changes in the mosaic structure (due to the nucleation of the B2 phase including in the B1 matrix) below and near the actual transition point and gave some insights into the mechanisms involved in the transformation. Based on the results of these experimental investigations, a model for the initial stages of the B1 to B2 transition in RbI was put forward⁽³⁶⁾. The main idea of the model is centered around the fact that the B1 structure can transform to the B2 structure by a collective translation of ions in the B1(0,0,1) alternative planes. This qualitative mechanism put forward describes an inhomogeneous transformation, which starts in regions of high dislocation densities. Furthermore, it was shown that a transformation hysteresis depending on the previous thermal and mechanical treatments of the sample and implying an actual transformation pressure different from the thermodynamic equilibrium point. However many aspects of this phenomenon have not been theoretically understood.

Recent advance in the method of computer simulation of solids make us to believe that a new molecular dynamic method developed by Parrinello and Rahman⁽³⁷⁾ may shed light on the manner in which the system of interest traverses its configuration space to achieve a polymorphic transition.

Parrinello and Rahman^[38] applied their new computational method to the polymorphic transition of KCl using a parameterized form of the Gordon-Kim potential^[27]. The calculation was described in details to show the dynamical history of the occurrence of a B1 to B2 transition. A new microscopic mechanism has been proposed to describe the accompanying changes in particle position in details. It should be noticed that the two proposed microscopic mechanism of the B1 to B2 transition— one proposed by Parrinello and Rahman based on their MD studies; the other by Blaschko et al. based on their experimental studies— coincide with each other, even though described independently in different manners.

Parrinello and Rahman pointed out that the B1 to the B2 transition can be described as a phonon softening associated with a spontaneous uniaxial deformation of the crystal. However the pressure and temperatures needed to accomplish the transformation on the computer simulation were much larger than those experimentally observed and in disagreement with the predictions made by Boyer⁽²⁸⁾ on the basis of a harmonic free energy calculation that used the same Gordon-Kim potential. This lead us to believe that a correct description of the transitions requires not only an accurate evaluation of the free energy difference between the two phases but also a reasonable estimate of the energy barriers that hinder the transition.

The work of Parrinello and Rahman describes the path in the configuration space that the system follows in going from one phase into the other. Thus we are now in the position to evaluate the free energy barriers and the effect on them of various choices of the potential and of the presence of defects that can help nucleating the different phases.

As alluded to before the mechanism of the B1 to B2 transition has been described by Parrinello and Rahman⁽³⁸⁾ as an uniaxial $[0, 1, 1]$ deformation of the B1 structure plus a softening of a transvers $[1, 0, 0]$ phonon mode. A full calculation of the free energy variation along this path is obviously a difficult task, thus we will confine ourselves to use of the harmonic approximation. Furthermore we will achieve the effect of deforming the B1 structure in the $[0, 1, 1]$ direction by a convenient uniaxial tensile load.

In our preliminary static study, a uniaxial loading was applied to KCl crystal in addition to a hydrostatic pressure. Our main aims are as follows: to investigate how the system evolves its configuration to reach a instable point after which the transition may follow; how the height of the free energy barrier varies with the thermonamic parameters. We will present the results of the zero temperature case neglecting the harmonic vibrations. This study will naturelly be extended to including the effects of the harmonic vibrations in the cases of the zero and finite temperatures.

The organization of this theses is as follows. Section 2 discusses some geometrical aspects of the B1 and B2 structures concerning the microscopic mechanism of polymorphic transitions in alkali halides. In section 3 a brief review of the MD method will be introduced. In section 4 our static calculation, as mentioned above , will be presented.. In the concluding remarks we will briefly outline our new study directions.

II. Some Geometrical Aspects of B1 and B2 Structure

It is convenient to gather together here a number of geometrical considerations of the B1 and B2 structures, which are utilized throughout the theses, as a starting point of our discussion. A detailed description can be found in textbooks [44]-[45]. We are dealing with cohesive property of Alkali halides under various external conditions, both distorted and undistorted configurations should be discussed. Some microscopic mechanism of the B1 to B2 transformation will be described in details.

(1) Crystal Structure of B1 and B2 Phase

B1 (or B2) structure is composed of two interpenetrating face-centered cubic (or simple cubic) Bravais lattices. With reference to the cube axes the B1 (or B2) structure is composed of two fcc (or SC) lattices, one for each species of ions, shifted by $a(\frac{1}{2}, \frac{1}{2}, \frac{1}{2})$ relative to one another, as illustrated in Fig1. The fundamental translation vectors of the fcc lattice are

$$\vec{a}_1 = a(0, \frac{1}{2}, \frac{1}{2}), \quad \vec{a}_2 = a(\frac{1}{2}, 0, \frac{1}{2}), \quad \vec{a}_3 = a(\frac{1}{2}, \frac{1}{2}, 0), \quad (2.1)$$

and these of the SC lattice are

$$\vec{a}_1 = a(1, 0, 0), \quad \vec{a}_2 = a(0, 1, 0), \quad \vec{a}_3 = a(0, 0, 1). \quad (2.2)$$

The reciprocal lattices of the fcc and SC Bravais lattices are body-centered cubic and simple cubic lattices respectively.

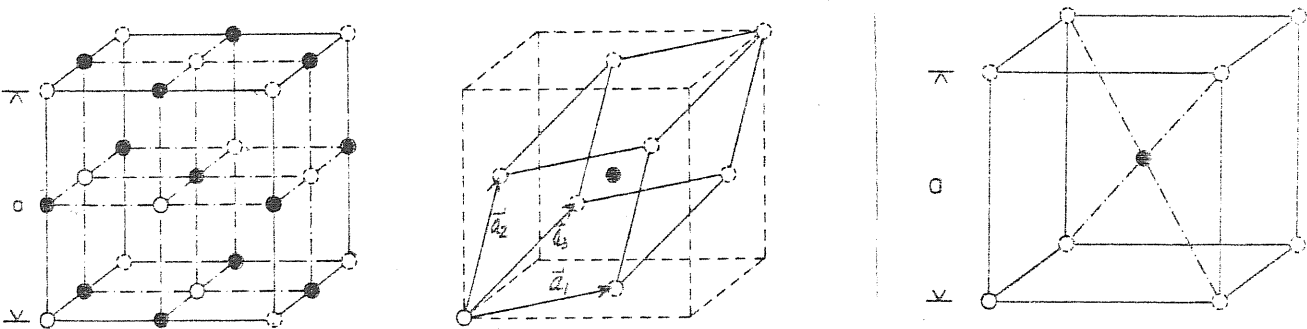


Fig.1. (a) A lattice cell and (b) a unit cell of the B1 structure. (c) A unit cell of the B2 structure. The blackened circle and the continuous circle represent the ions of the cell.

With reference to the cube axes, their fundamental translation vector are given by

$$\vec{a}_1^* = \frac{2\pi}{a}(-1, 1, 1), \quad \vec{a}_2^* = \frac{2\pi}{a}(1, -1, 1), \quad \vec{a}_3^* = \frac{2\pi}{a}(1, 1, -1), \quad (2.3)$$

and by

$$\vec{a}_1^* = \frac{2\pi}{a}(1, 0, 0), \quad \vec{a}_2^* = \frac{2\pi}{a}(0, 1, 0), \quad \vec{a}_3^* = \frac{2\pi}{a}(0, 0, 1), \quad (2.4)$$

respectively. Fig.2 shows the associated first Brillouin Zones. We have indicated on these figures the various symmetry points and symmetry axes. The notation follows that of Bouckaerd, Smoluchowski and Wigner^[48]. Different structure may be characterized by ionic shells with certain shell distance and coordination numbers. Table 1 gives the comparison between B1 and B2 structures.

In the table the first line gives the nearest neighbor distances. Denoting ion coordinate by (x,y,z) in $\frac{1}{2}a$ units, note that different type of ions has different parities of $x+y+z$ for both cases of B1 and B2 structure. In $\frac{1}{2}a$ units, x,y,z can be any integer for B1 structure; should be simultaneously even or simultaneously odd numbers for B2 structure.

Table 1: Ionic shells of B1 and B2 structure

B1 structure			B2 structure		
Ion coordinates (in $\frac{1}{2}a$ unit)	Number of ions	Distance from(0,0,0) (in $\frac{1}{2}a$ unit)	Ion coordinates (in $\frac{1}{2}a$ unit)	Number of ions	Distance from(0,0,0) (in $\frac{1}{2}a$ unit)
(1,0,0)	6	1	(1,1,1)	8	1
(1,1,0)	12	$\sqrt{2}$	(2,0,0)	6	$\frac{2}{3}\sqrt{3}$
(1,1,2)	8	$\sqrt{3}$	(2,2,0)	12	$\frac{2}{3}\sqrt{6}$
(2,0,0)	6	2	(2,2,2)	8	2
(2,1,0)	24	$\sqrt{5}$	(3,1,1)	24	$\frac{1}{3}\sqrt{33}$
(2,1,1)	24	$\sqrt{6}$	(3,3,1)	24	$\frac{1}{3}\sqrt{57}$
(2,2,0)	12	$2\sqrt{2}$	(3,3,3)	8	3
(2,2,1)	24	3	(4,0,0)	6	$\frac{4}{3}\sqrt{3}$
(2,2,2)	8	$2\sqrt{3}$	(4,2,0)	24	$\frac{2}{3}\sqrt{15}$
(3,0,0)	6	3	(4,2,2)	24	$2\sqrt{2}$
(3,1,0)	24	$\sqrt{10}$	(4,4,0)	12	$\frac{4}{3}\sqrt{6}$
(3,1,1)	24	$\sqrt{11}$	(4,4,2)	24	$2\sqrt{3}$
(3,2,0)	24	$\sqrt{13}$	(4,4,4)	8	4
.....					

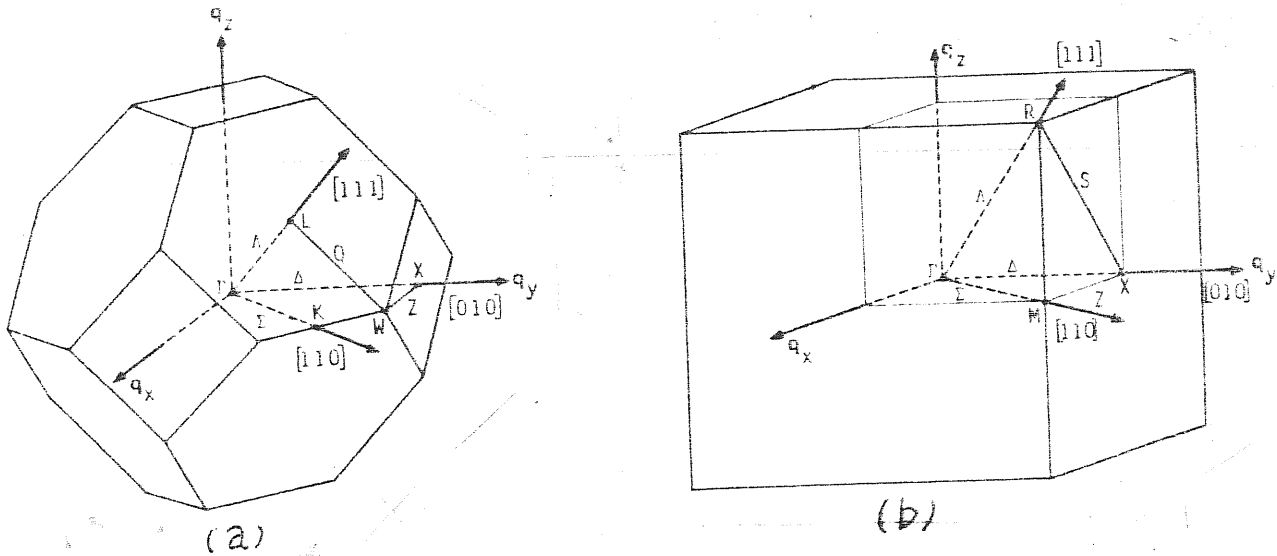


Fig.2. Brillouin zones for (a) face-centered cubic (b) simple cubic lattices.

(2) Relationship between B1 and B2 structure, a discussion on microscope mechanism of transformation from B1 to B2 structure.

Shoji [29] pointed out the possibility of a relative expansion along one of the threefold axes for transforming the B2 lattice to the B1, but did not consider this a realistic explanation. However this mechanism was illustrated by Buerger [30]. As shown in Fig1(b) and (c), the unit cell of the B2 structure can be obtained from the unit cell of B1 structure by a contraction along the (111) axis and expansion at right angles to this axis. This deformation maintains the contact of the six ions at the face centers with the ion at the cube center, while it brings the two ions on the cube corners in contact with it. It was conjectured that the change occurred by a trigonal lattice of angle 60° which is a fcc lattice; becoming a trigonal lattice of angle 90° which is a simple cubic lattice. The deformation consists of a uniform contraction and a set of C_{44} type shear strains [47]. Hardy and Karo [48] indicated that B1 structure can be forced to become unstable for short wave length vibrations in the (1,0,0) transverse acoustic branch.

Mennry et.al.[49] were the first to use single crystals to study the orientation relation in the transition of CsCl by means of an X-ray diffraction method. The existence of definite orientation of B1 (1,0,0) B2 (1,1,0) in the transition between the B1 and B2 structure was reported by a number of investigators [50],[31-32]. Fraser and Kennedy [31] has proposed that this transition is cooperative. Furthermore Watanabe et al [32] put forward a transition mechanism, which is explained as being due to a combination of two systematic movement of ions: intralayer rearrangement and interlayer translation. As shown in Fig 3. This mechanism was supported by the fact that a uniaxial expansion paralleled to one of the twofold axes in the B2 structure (or the fourfold axes in the B1 structure) attending the transition was observed under the optical microscope.

Recently Blaschko et.al.[36] pointed out that in the B1 and in the B2 structure two crystallographic planes, i.e. B1 (0,0,1) and B2 (1,1,0) are topologically rather similar. Without changing the occupation of the lattice site the B1 (0,0,1) plane can be transformed to the B2 (1,1,0) plane by simply adjusting

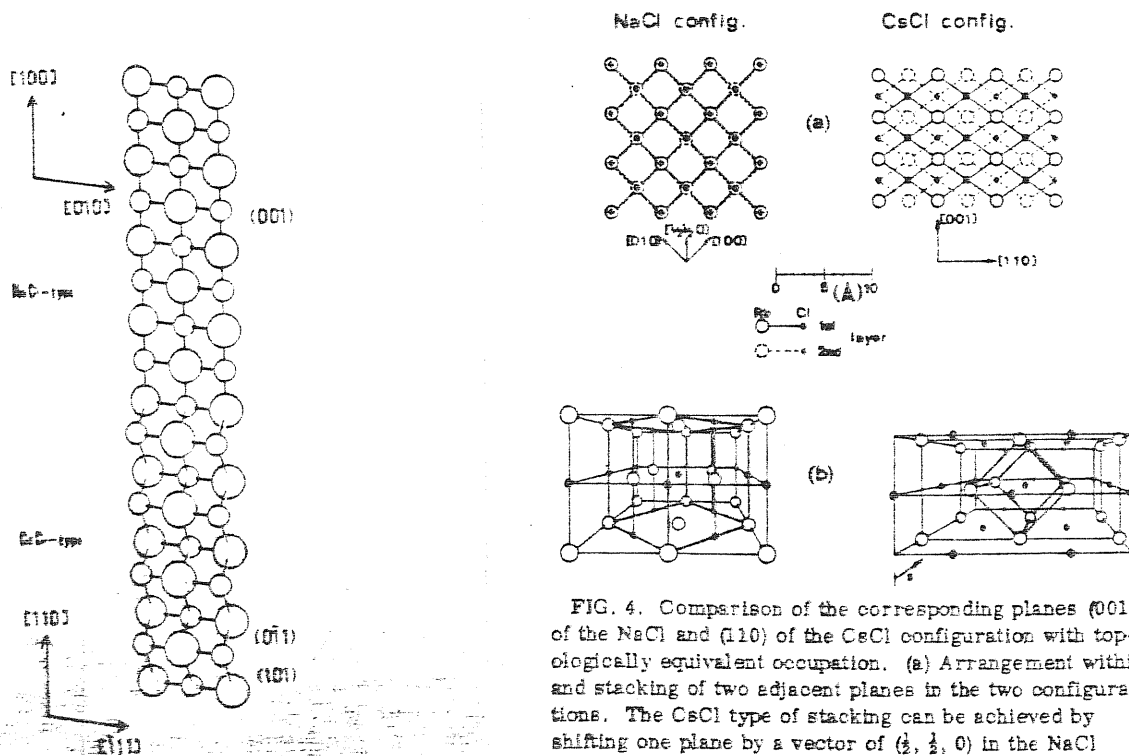


Fig. 3 Change of the zigzag plane consisting of (101) and (011) of the CsCl-type structure to the flat plane of (001) of the NaCl-type structure resulting in the uniaxial expansion in the transition.

FIG. 4. Comparison of the corresponding planes (001) of the NaCl and (110) of the CsCl configuration with topologically equivalent occupation. (a) Arrangement within and stacking of two adjacent planes in the two configurations. The CsCl type of stacking can be achieved by shifting one plane by a vector of $(\frac{1}{2}, \frac{1}{2}, 0)$ in the NaCl configuration. (b) Three-dimensional plot of the two configurations. The unit cells are drawn with bold lines. The difference in the stacking is indicated by the vector \vec{S} .

the distances between the atoms (Fig 4(a)). In the real transformation, therefore, an $B1(0,0,1)$ plane can transform to an $B2(1,1,0)$ plane by rearranging the atomic distances in the planes. The presence of the orientation relation $B1(0,0,1) \parallel B2(1,1,0)$ in the transformation shows the importance of this correspondence of the transformation mechanism, which has been discussed in the section 1, is illustrated in Fig 4. This mechanism was based on the following experimental facts:

(a) The transformation is inhomogeneous, i.e. well defined $B2$ inclusions appear, whereas the $B1$ matrix is still present [20].

(b) The occurrence of a strong orientation relation between the two phase, i.e. $B1(0,0,1) \parallel B2(1,1,0)$ [20].

(c) Phonon frequency anomalies occur for transverse-acoustic phonons mainly for the $TA(0,0,\frac{1}{2})$ branch [20].

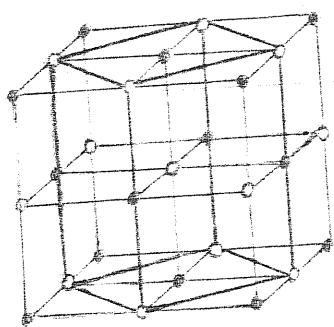
It was proposed that the occurrence of collective shift of ions in the alternative $B1(0,0,1)$ planes described by a translation $(\frac{1}{2}, \frac{1}{2}, 0)$ vector, which may be created by a shear transformation, should influence the phonon frequencies, especially those of the $TA(0,0,\frac{1}{2})$ branch with a polarization in the $(1,1,0)$ direction.

Experimental results show that real mechanism for various transition may be intricate, while systematic theoretical investigation is till lacking.

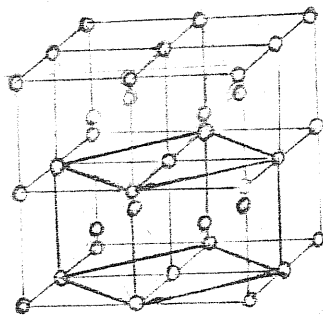
As mentioned in the section 1, the mechanism proposed by Blaschko, et. al, coincides in a mechanism based on theoretical investigation of Parrinello and Rahman [38].

Parrinello and Rahman pointed out that it is important to understand the following geometrical fact when study the structure transformations. As shown in Fig5, a body centered tetragonal lattice with edges $1, 1, \sqrt{2}$ is an fcc structure and inversely a tetragonal faced centered lattice with edges $\sqrt{2}, \sqrt{2}, 1$ is a bcc structure. Moreover, a tetragonal based centered lattice with edges $\sqrt{2}, \sqrt{2}, 1$ is a sc structure, if the square face is specified as the base.

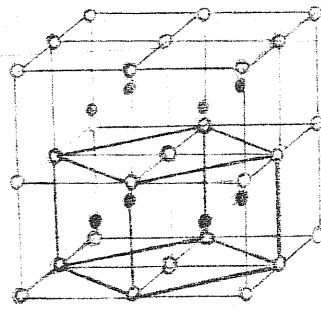
Based on the new MD calculation for $B1$ to $B2$ transformation of KCl , Parrinello and Rahman [38] have presented a microscopic mechanism of the transformation. A particle by particle analysis of the transformation reveals how the $B1$ to $B2$ transformation occurs (Fig.6).



(a)



(b)



(c)

Fig.5. (a) B1 structure, a body centered tetragonal lattice with a basis consisting of a ion at the origin and a oppositely charged ion at the center of a square face; (b) b.c.c. lattice; (c) B2 structure, a base centered tetragonal lattice with a basis consisting of a ion at the origin and a oppositely charged ion at the center of a rectangle face.

Fig.6A shows a body-centered tetragonal lattice, lattice vectors $\vec{a}, \vec{b}, \vec{c}$, length $a, a, \sqrt{2}a$ respectively. The atoms are indicated by \bullet . This is an fcc lattice of \bullet ions. The other species, shown as \circ , completes the B1 structure.

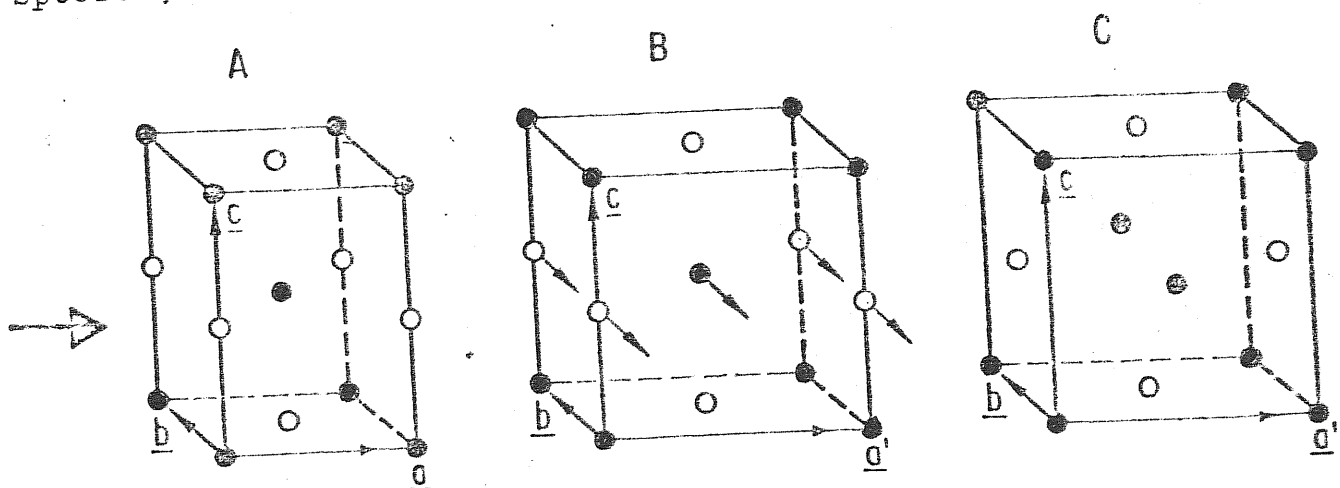


Fig.6: Detail of rocksalt to cesium chloride found to occur in this calculation. [38] Thick arrow in A indicates a dilatation, resulting in B. Fine arrows in B indicate displacements of particles with a common c direction coordinate, resulting in the final structure C. A is a B1 and C a B2 structure.

Operation # 1: Uniform dilatation of amount $\sqrt{2}$ in the direction of a as indicated by the thick arrow in Fig.6A. The result is shown in Fig.6B $\vec{a}, \vec{b}, \vec{c}$ become $\vec{a}', \vec{b}, \vec{c}$.

Operation # 2: A move of alternate planes in the \vec{c} direction as indicated by the fine arrows in Fig.6B. The result is shown in Fig.6C; the center of the square face formed by \vec{a}, \vec{c} is now occupied by \bullet . An atom of the same type occupies the opposite square face, it is the shadowing filled circle in Fig.6C.

Fig.6C shows a simple cubic lattice of like ions, the like and unlike ions together forming a B2 structure as indicated in Fig.5c.

(3) The face-centered tetragonal lattice (f,c,t) and deformed f,c,t, lattice.

The microscopic mechanism of B1 to B2 transformation discussed in ^{the}last subsection implies that in ^{the}general cases f.c.c. lattice will be deformed to be f.c.t lattice or deformed f.c.t lattice. The basic vectors of crystallographic unit cell are shown in Fig.7.

(a) The simple tetragonal lattice (s,t).

In rectangular coordinate the basic vector for the direct and reciprocal lattices are given by

$$\vec{b}_1 = a(\lambda_1, 0, 0), \quad \vec{b}_2 = a(0, \lambda_2, 0), \quad \vec{b}_3 = a(0, 0, \lambda_2), \quad (2.5)$$

$$\vec{b}_1^* = \frac{2\pi}{a} \left(\frac{1}{\lambda_1}, 0, 0 \right), \quad \vec{b}_2^* = \frac{2\pi}{a} \left(0, \frac{1}{\lambda_2}, 0 \right), \quad \vec{b}_3^* = \frac{2\pi}{a} \left(0, 0, \frac{1}{\lambda_2} \right), \quad (2.6)$$

and $\vec{b}_i \cdot \vec{b}_j = 2\pi \delta_{ij}$. The direct lattice point is expressed as $R_m = m_1 \vec{b}_1 + m_2 \vec{b}_2 + m_3 \vec{b}_3 = [m_1, m_2, m_3]$ with m_1, m_2, m_3 any integers. A general point in the B.Z may be expressed as $K = u\vec{b}_1^* + v\vec{b}_2^* + w\vec{b}_3^* = [u, v, w]$, K would be a reciprocal lattice vector if u, v, w are all integers.

(b) The face-centered tetragonal lattice (f.c.t).

In rectangular coordinate systems, the basic vector for the direct and reciprocal lattices are ^{as} follows:

$$\vec{B}_1 = \frac{a}{2} (0, \lambda_2, \lambda_2), \quad \vec{B}_2 = \frac{a}{2} (\lambda_1, 0, \lambda_2), \quad \vec{B}_3 = \frac{a}{2} (\lambda_1, \lambda_2, 0), \quad (2.7)$$

$$\vec{B}_1^* = \frac{2\pi}{a} \left(-\frac{1}{\lambda_1}, \frac{1}{\lambda_2}, \frac{1}{\lambda_2} \right), \quad \vec{B}_2^* = \frac{2\pi}{a} \left(\frac{1}{\lambda_1}, -\frac{1}{\lambda_2}, \frac{1}{\lambda_2} \right), \quad \vec{B}_3^* = \frac{2\pi}{a} \left(\frac{1}{\lambda_1}, \frac{1}{\lambda_2}, -\frac{1}{\lambda_2} \right). \quad (2.8)$$

However, it is convenient to express the direct and reciprocal

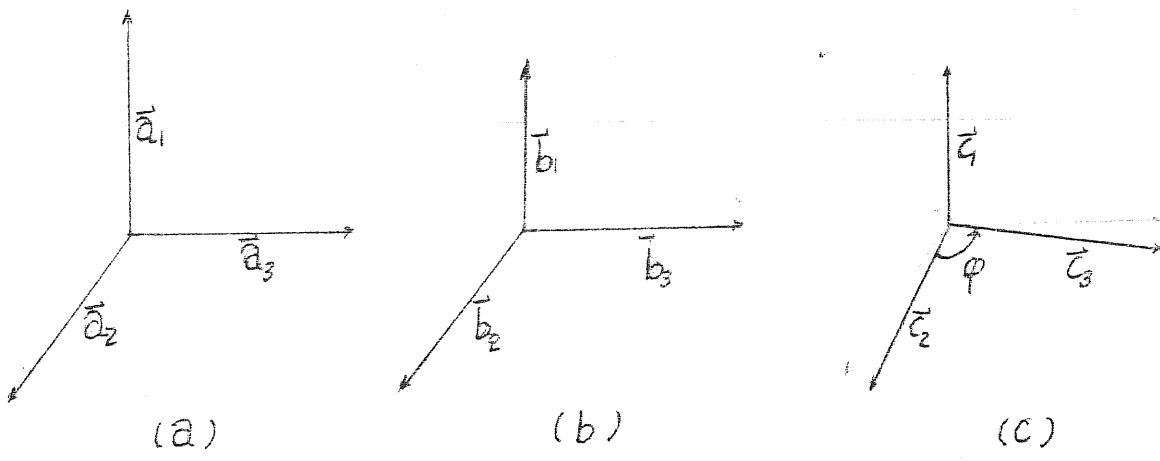


Fig.7. Schematic representation to show that (a) $\vec{a}_1, \vec{a}_2, \vec{a}_3$ span crystallographic unit cell of fcc lattice with $|\vec{a}_1| = |\vec{a}_2| = |\vec{a}_3| = a$ and $\vec{a}_1 \perp \vec{a}_2 \perp \vec{a}_3$; it is a simple cubic (b) $\vec{b}_1, \vec{b}_2, \vec{b}_3$ span that of f.c.t lattice with $|\vec{b}_3| = |\vec{b}_2| = \lambda_2 a, |\vec{b}_1| = \lambda_1 a, \lambda_2 \neq \lambda_1$ and $\vec{a}_1 \perp \vec{a}_2 \perp \vec{a}_3$; it is a simple tetragonal; (c) $\vec{c}_1, \vec{c}_2, \vec{c}_3$ span that of deformed f.c.t lattice with $|\vec{c}_2| = |\vec{c}_3| = \lambda_2 a, |\vec{c}_1| = \lambda_1 a, \lambda_2 \neq \lambda_1$, and $\vec{c}_1 \perp \vec{c}_3, \vec{c}_1 \perp \vec{c}_2$, but $\varphi \neq 90^\circ$.

lattice vector of the f.c.t in terms of the basis vectors in S.T. This gives $\vec{R}_m = M_1 \vec{B}_1 + M_2 \vec{B}_2 + M_3 \vec{B}_3 = m_1 \vec{b}_1 + m_2 \vec{b}_2 + m_3 \vec{b}_3 = [m_1, m_2, m_3]$ with m_1, m_2, m_3 any integers simultaneously or one is a integer and the other are odd integers divided by 2. A general point in the B.Z is $K = u\vec{B}_1^* + v\vec{B}_2^* + w\vec{B}_3^* = u\vec{b}_1^* + v\vec{b}_2^* + w\vec{b}_3^* = [u, v, w]$. K becomes a reciprocal lattice vector when u, v, w are simultaneously even integers or simultaneously odd integers.

The volume of primitive unit cell is

$$V = \frac{1}{2} \lambda_1 \lambda_2^2 a^3. \tag{2.9}$$

When the crystallographic cell of B1 structure is deformed to be f.c.t lattice, the basic vector are

$$\begin{aligned} \vec{r}_{t_1} &= (0, 0, 0), & q_{t_1} &= -1, \\ \vec{r}_{t_2} &= \frac{a}{2} (\lambda_1, \lambda_2, \lambda_2), & q_{t_2} &= 1, \end{aligned} \tag{2.10}$$

each basic vector \vec{r}_{t_i} associates a point charge q_{t_i} respectively. The structure factor is

$$S(\vec{K}) = \sum_t q_t e^{-\vec{K} \cdot \vec{r}_t}$$

$$= \begin{cases} -2, & \text{if } u, v, w \text{ are simultaneously odd,} \\ 0, & \text{otherwise.} \end{cases} \quad (2.11)$$

(c) The deformed face-centered tetragonal lattice.

In rectangular coordinate systems, the basis vector for the direct and reciprocal lattices are given by

$$\begin{aligned} \vec{A}_1 &= \frac{\sqrt{2}}{2} \pi_2 a \cos \frac{\varphi}{2} (0, 1, 1), \\ \vec{A}_2 &= \frac{a}{2} (\pi_1, \frac{\pi_2}{\sqrt{2}} (\cos \frac{\varphi}{2} - \sin \frac{\varphi}{2}), \frac{\pi_2}{\sqrt{2}} (\cos \frac{\varphi}{2} + \sin \frac{\varphi}{2})), \\ \vec{A}_3 &= \frac{a}{2} (\pi_1, \frac{\pi_2}{\sqrt{2}} (\cos \frac{\varphi}{2} + \sin \frac{\varphi}{2}), \frac{\pi_2}{\sqrt{2}} (\cos \frac{\varphi}{2} - \sin \frac{\varphi}{2})), \end{aligned} \quad (2.12)$$

$$\begin{aligned} \vec{A}_1^* &= \frac{2\pi}{a} \left(-\frac{1}{\pi_1}, \frac{\sqrt{2}}{2\pi_2 \cos \frac{\varphi}{2}}, \frac{\sqrt{2}}{2\pi_2 \cos \frac{\varphi}{2}} \right), \\ \vec{A}_2^* &= \frac{2\pi}{a} \left(\frac{1}{\pi_1}, \frac{-\sqrt{2}}{2\pi_2 \sin \frac{\varphi}{2}}, \frac{\sqrt{2}}{2\pi_2 \sin \frac{\varphi}{2}} \right), \\ \vec{A}_3^* &= \frac{2\pi}{a} \left(\frac{1}{\pi_1}, \frac{\sqrt{2}}{2\pi_2 \sin \frac{\varphi}{2}}, \frac{-\sqrt{2}}{2\pi_2 \sin \frac{\varphi}{2}} \right). \end{aligned} \quad (2.13)$$

Note that if $\varphi = 90^\circ$, i.e. $\cos \varphi = 0$, (2.12) and (2.13) would coincide in equation (2.7) and (2.8) respectively; and if $\pi_1 = \pi_2 = 1$ and $\cos \varphi = 0$, (2.12) and (2.13) become equation (2.1) and (2.3) respectively. It is convenient to express the direct and reciprocal lattice vector of the deformed f.c.t in terms of the basis vectors $\vec{c}_1, \vec{c}_2, \vec{c}_3$ and $\vec{c}_1^*, \vec{c}_2^*, \vec{c}_3^*$ in deformed s.t. as shown in Fig.7(c), where

$$\begin{aligned} \vec{c}_1 &= (\pi_1 a, 0, 0), \\ \vec{c}_2 &= (0, \pi_2 a \frac{\sqrt{2}}{2} (\cos \frac{\varphi}{2} + \sin \frac{\varphi}{2}), \pi_2 a \frac{\sqrt{2}}{2} (\cos \frac{\varphi}{2} - \sin \frac{\varphi}{2})), \\ \vec{c}_3 &= (0, \pi_2 a \frac{\sqrt{2}}{2} (\cos \frac{\varphi}{2} - \sin \frac{\varphi}{2}), \pi_2 a \frac{\sqrt{2}}{2} (\cos \frac{\varphi}{2} + \sin \frac{\varphi}{2})), \end{aligned} \quad (2.14)$$

and

$$\begin{aligned} \vec{c}_1^* &= \frac{2\pi}{a} \left(\frac{1}{\pi_1}, 0, 0 \right), \\ \vec{c}_2^* &= \frac{2\pi}{a 2 \sin \varphi} \left(0, \frac{\cos \frac{\varphi}{2} + \sin \frac{\varphi}{2}}{\pi_2}, \frac{-(\cos \frac{\varphi}{2} - \sin \frac{\varphi}{2})}{\pi_2} \right), \\ \vec{c}_3^* &= \frac{2\pi}{a 2 \sin \varphi} \left(0, \frac{-(\cos \frac{\varphi}{2} - \sin \frac{\varphi}{2})}{\pi_2}, \frac{\cos \frac{\varphi}{2} + \sin \frac{\varphi}{2}}{\pi_2} \right), \end{aligned} \quad (2.15)$$

with

$$\vec{c}_i \cdot \vec{c}_j^* = 2\pi \delta_{ij}. \quad (2.16)$$

This gives $\vec{R}_m = M_1 \vec{A}_1 + M_2 \vec{A}_2 + M_3 \vec{A}_3 = m_1 \vec{c}_1 + m_2 \vec{c}_2 + m_3 \vec{c}_3 = [m_1, m_2, m_3]$ with m_1, m_2, m_3 are simultaneously integer or one is a integer and the other two are odd integers divided by two. A general point in the B.Z. is $\vec{K} = U\vec{A}_1^* + V\vec{A}_2^* + W\vec{A}_3^* = u\vec{c}_1^* + v\vec{c}_2^* + w\vec{c}_3^* = [u, v, w]$. If u, v, w are simultaneously even or simultaneously odd integers, then \vec{K} is a reciprocal lattice vector.

The volume of primitive unit cell is

$$V = \frac{1}{2} \pi_1 \pi_2 a^3 \sin \varphi, \quad (2.17)$$

The basic vectors in this case are

$$\vec{r}_{t_1} = (0, 0, 0), \quad q_{t_1} = -1; \quad (2.18)$$

$$\vec{r}_{t_2} = \frac{a}{2} (\pi_1, \sqrt{2}\pi_2 \cos \frac{\varphi}{2}, \sqrt{2}\pi_2 \cos \frac{\varphi}{2}), \quad q_{t_2} = 1.$$

If we express the reciprocal lattice vector by K

$$\vec{K} = U\vec{A}_1^* + V\vec{A}_2^* + W\vec{A}_3^*,$$

the structure factor is

$$S(K) = \sum_t q_t e^{-i\vec{K} \cdot \vec{r}_t} = \begin{cases} -2, & \text{if } U+V+W \text{ is odd integer,} \\ 0, & \text{otherwise.} \end{cases} \quad (2.19)$$

To enclose this subsection we show that the configuration corresponding to Fig. 6B is a deformed f.c.t lattice specified by parameters π_1, π_2 and $\cos \varphi$, with $\pi_2 = 1.2247\pi_1, \cos \varphi = 0.3333$, i.e. $\varphi = 70.53^\circ$. This configuration generally can be obtained by simultaneously dilation on (0, 1, 1) direction and suppression on (1, 0, 0) direction.

III. New Molecular Dynamics Method

In the past decade or more molecular dynamics (MD) and Monte Carlo (MC) calculations have become widely used techniques for the study of condensed systems. Their importance rests largely on the fact that they provide essentially exact, quasiexperimental data on well-defined models. Moreover it is possible to obtain information on quantities of theoretical importance which cannot easily be measured in the laboratory. A brief account was given by Hansen and McDonald.^[51] Molecular dynamics has the advantage of allowing the study of time-dependent phenomena. Our concern will be only with MD method. The salient features of the MD technique was outlined in the lectures given by Rahman.^[52]

The first molecular dynamics calculation were made by Alder and Wainwright^{[53], [54]}. The application of MD to realistic systems was first described by Rahman^{[55], [56]} and was extended by a large number of investigators^{[57]-[60]}. Even though the largest amount of effort has gone into the study of fluids, considerable work on perfect solids at high temperature has also been done. A detailed account of work on molten alkali halides was given by Sangster and Dixon^[61]. It should be remarked here that a study of the traditional MD technique, which has been confined to a perfect and prefixed crystalline arrangement of the atoms.

It has now become possible to study this structure change by computer simulation. Recent work of Parrinello and Rahman^[37] has show that by using an appropriate Lagrangian one can set up a molecular dynamics calculation in which both the volume and the shape of the periodically repeating cell change with time. They have demonstrated^[37] the utility of these new dynamical equation by applying them to simple monatomic systems and showed if a system of Lennard-Jones atoms is given a bcc structure then under suitable density, temperature conditions the dynamical equations themselves make the system change its structure to a close packed one. Applying this new MD method to polymorphic transitions in single crystals^[39] showed that this method is pertinent to the discussion of the behaviour of solids under the combined effects of external stress and of temperature.

In thier study of polymorphic transition in KCl [38], a microscopic mechanism of B1 to B2 transformation has been revealed. Parrinello, Rahman and Vashishta [62],[63] have used this new technique to study structural transformation in AgI. It shows that new MD method is really a powerfull tool for study structure transition in solids.

We shall first give a brief description of the tranditional MD method before looking in more detail at the new MD method.

(1) A Brief Survey on Tranditional MD Method.

In the MD simulation the Newtonian equation of motion of a set of N particle are solved numerically. The particles interact through a potential $V_N(r_1, \dots, r_N)$ which, in most investigations is taken to be

$$V_N = \frac{1}{2} \sum_i \sum_j \Phi(r_{ij}), \quad (3.1)$$

where $r_{ij} = |r_{ij}| = |r_i - r_j|$ and r_i is the coordinates of the particle i. Newton's equations are then

$$m_i \ddot{r}_i = \sum_{j \neq i} \frac{1}{r_{ij}} \frac{d\Phi}{dr_{ij}} \hat{r}_{ij}, \quad i=1,2,\dots,N, \quad (3.2)$$

where m_i is the mass of particle i.

To solve these equation one needs to specify initial positions and velocities of all the particles. The problem is to convert the differential equations into a set of difference equation by using a suitably chosen algorithm ^{64,57} for the numerical integrations. The initial values for the velocities of the N particles are chosen to be subjected to the conatraint on the total momentum

$$\sum_{i=1}^N m_i \dot{r}_i = 0, \quad (3.3)$$

and scaled to give the temperature in the correct range

$$T = \frac{1}{3NK_B} \sum_{i=1}^N m_i \dot{r}_i^2, \quad (3.4)$$

The initial positions are chosen to be on a regular array of points of suitable geometry or as above with suitably randomized small displacements, avoiding situations of extremely large potential energy.

In simulating a bulk system the common practice is to use periodic boundary conditions which have the merit of removing

the surface effects in a mathematically well defined manner. These are obtained by periodically repeating a unit cell of volume Ω containing the N particles by suitable translations. Periodic boundary conditions obviously give a system in which the N particles are always contained in a cell of volume Ω , and without loss of generality every particle can be thought of as being at the "center". In other words, the summation over j in Eq (3.2) extends over the infinite system generated by the periodic boundary conditions.

The integration of the Eq(3,2) then gives the trajectories of all particles for subsequent (and earlier!) times. As the system evolves in time it eventually reaches equilibrium conditions in its dynamical and structure properties; the statistical averages of interest are calculated from $\vec{r}_i(t)$ and $\dot{\vec{r}}_i(t)$, $i=1, \dots, N$, as temporal averages over the trajectory of the system in its phase space.

$$A = \lim_{\tau \rightarrow \infty} \frac{1}{\tau} \int_0^\tau A(\vec{r}_1(\tau'), \dots, \vec{r}_N(\tau'); \dot{\vec{r}}_1(\tau'), \dots, \dot{\vec{r}}_N(\tau')) d\tau' \quad (3.5)$$

As a consequence of V_N being a function of r_i only, the solution of Eq(3.2) conserves the total energy E of the system:

$$E = \frac{1}{2} \cdot 3NkT + V_N = \text{const.} \quad (3.6)$$

This conservation condition can be used as a criterion for judging the accuracy of the trajectories generated.^[63] Thus the statistical ensemble generated in a conventional MD calculation is a (Ω, E, N) ensemble or a microcanonical ensemble.

A detailed survey on the MD technique was given by Rahman. Some of physical properties (of molten alkali halides) giving definitions and indicating the methods of MD calculation were listed by Sangster and Dixon.^[61] Here also a discussion on performing the Ewald sum for the energy and forces due to Coulomb interactions by using Singer's method can be found. The spirit of Singer's method was reviewed by Rahman and Vashishta^[62] in details.

The restriction that the MD cell be kept constant in volume and in shape severely restricts the applicability of the method to problems involving crystal structure transformation. In order to overcome this difficulty Andersen^[65] have presented a method allowing for changes in volume of the MD cell but not in its shape. Thus crystal structure transformations are inhibited in Andersen's method.

(2) New Molecular Dynamics Method.

For a study of the structural phase transformations it is essential to incorporate changes as a function of time in the volume as well as the shape of the cell within the framework of molecular dynamics technique. It has become possible to study this structure changes by using new MD method developed by Parrinello and Rahman.^[27] We will follow their original papers to give a brief review of this method.

In this new MD method a new Lagrangian formulation is introduced; it can be used to make molecular dynamical calculation on systems under the most general, externally applied condition of stress. In this formulation the MD cell shape and size can change according to dynamical equations given by this Lagrangian. This new MD technique is well suited to the study of structural transformations in solids under external stress and at finite temperature.

A time-dependent metric tensor was introduced, it allows the volume and the shape of the MD cell to vary with time.

Let the edges of the MD cell be $\vec{a}, \vec{b},$ and \vec{c} (in a spaced fixed coordinate system), and let them be time dependent. Periodically repeating MD cells will fill up all space. Let \underline{h} be the matrix formed by $\{\vec{a}, \vec{b}, \vec{c}\}$; $\Omega = \text{deth} \underline{h} = \vec{a} \cdot \vec{b} \times \vec{c}$ is the volume of the MD cell containing N particles. The position of particle i will be $\vec{r}_i = \xi_i \vec{a} + \eta_i \vec{b} + \zeta_i \vec{c} = \underline{h} \vec{s}_i$, where \vec{s}_i has components (ξ_i, η_i, ζ_i) each going from 0 to 1. Obviously $r_i^2 = \vec{s}_i' \underline{G} \vec{s}_i$, where $\underline{G} = \underline{h}' \underline{h}$ is the metric tensor, the transpose being denoted by a prime.

(A). The case when only hydrostatic pressure is applied

In Ref(37) variability in the shape and size of the MD cell was obtained as follows: the usual set of 3N dynamical variables, that describe the positions of the N particles, was augmented by the nine components of \underline{h} . The time evolution of the 3N+9 variables was then obtained from the Lagrangian

$$\mathcal{L} = \frac{1}{2} \sum_{i=1}^N m_i \dot{\vec{s}}_i' \underline{G} \dot{\vec{s}}_i - \sum_{i=1}^N \sum_{j \neq i} \Phi(r_{ij}) + \frac{1}{2} W \text{Tr} \dot{\underline{h}}' \dot{\underline{h}} - P \Omega \quad (3.7)$$

where P is the hydrostatic pressure. W has dimensions of mass.³⁹ The Lagrangian equations of motion can be written down :

$$\ddot{\vec{s}}_i = - \sum_{j=1}^N m_i^{-1} (\Phi'/r_{ij}) (\vec{s}_i - \vec{s}_j) - \underline{G}^{-1} \underline{\dot{G}} \vec{s}_i, \quad i=1, \dots, N \quad (3.8)$$

$$\underline{W} \underline{h} = (\underline{N} - P) \underline{\sigma} \quad (3.9)$$

Here $\Phi(r)$ is pair potential; The matrix $\underline{\sigma}$

$$\underline{\sigma} = \Omega \underline{h}^{-1} = \{ \vec{b} \wedge \vec{c}, \vec{c} \wedge \vec{a}, \vec{a} \wedge \vec{b} \} \quad (3.10)$$

carries information concerning the size and orientation of the MD cell. In equation (3.9), using the usual dyadic notation, and writing $\vec{v}_i = \underline{h} \dot{\vec{s}}_i$

$$\Omega \underline{N} = \sum_i m_i \vec{v}_i \vec{v}_i - \sum_i \sum_{j \neq i} (\Phi'/r_{ij}) \vec{r}_{ij} \vec{r}_{ij} \quad (3.11)$$

When $\underline{h} = \text{const.}$, i.e., when the MD cell is time independent, $\dot{\underline{G}} = 0$ and Eq(3.8) becomes identical to the Newton equation in the traditional MD method, i.e., Eq(3.2).

Note that the Lagrangian in Eq(3.7) generates a (P,H,N) ensemble, and here

$$H = E + P \quad (3.12)$$

$$E = \sum_i \frac{1}{2} m_i v_i^2 + \sum_i \sum_{j \neq i} \Phi(r_{ij}) \quad (3.13)$$

(B). The case when a general stress is applied

In order to make above framework to extend to the case when a general stress is applied, a reference state was introduced.^[39] This reference state of the system can be defined by its matrix \underline{h}_0 and volume $\Omega_0 = \|\underline{h}_0\|$. In this reference state a point in space given by the coordinate vector \vec{s} is at the position

$$\vec{r}_0 = \underline{h}_0 \vec{s} \quad (3.14)$$

A homogeneous distortion of the system changes \underline{h}_0 to \underline{h} , moving \vec{r}_0 to \vec{r} , where

$$\vec{r} = \underline{h} \vec{s} = \underline{h} \underline{h}_0^{-1} \vec{r}_0 \quad (3.15)$$

giving the displacement \vec{u} due to the distortion:

$$\vec{u} = \vec{r} - \vec{r}_0 = (\underline{h} \underline{h}_0^{-1} - \underline{1}) \vec{r}_0 \quad (3.16)$$

Following Landau and Lifshitz^[66] to define the strain and using x_μ to denote the components of \vec{r}_0

$$\epsilon_{\lambda\mu} = \frac{1}{2} \left(\frac{\partial u_\lambda}{\partial x_\mu} + \frac{\partial u_\mu}{\partial x_\lambda} + \sum \frac{\partial u_\lambda}{\partial x_\mu} \frac{\partial u_\mu}{\partial x_\lambda} \right) \quad (3.17)$$

The expression of $\underline{\epsilon}$ has been given by Parrinello and Rahman as follows:

$$\underline{\epsilon} = \frac{1}{2} (\underline{h}_0'^{-1} \underline{G} \underline{h}_0^{-1} - 1) \quad (3.18)$$

Having identified the strain $\underline{\epsilon}$, an expression for the elastic energy, V_{el} , can be now written. If \underline{S} is the external stress and p the hydrostatic pressure,

$$V_{el} = p(\Omega - \Omega_0) + \Omega_0 \text{Tr}(\underline{S} - p)\underline{\epsilon} \quad (3.19)$$

To generalize the Lagrangian of Eq(3.7), we need to substitute V_{el} of Eq(3.19) in place of $p\Omega$ in Eq(3.7) for \mathcal{L} . This gives us the new Lagrangian \mathcal{L}_S ,

$$\mathcal{L}_S = \mathcal{L} - \frac{1}{2} \text{Tr} \underline{\Sigma} \underline{\epsilon} \quad (3.20)$$

where the symmetric tensor $\underline{\Sigma}$ is related to the stress \underline{S} :

$$\underline{\Sigma} = \underline{h}_0'^{-1} (\underline{S} - p) \underline{h}_0^{-1} \quad (3.21)$$

Using Eq(3.20) to write the Lagrangian equations of motion we get Eq(3.8) as before but Eq(3.9) is now replaced by

$$\underline{W} \ddot{\underline{h}} = (\underline{\pi} - p) \underline{\sigma} - \underline{h} \underline{\Sigma} \quad (3.22)$$

It is easy to see that, analogous to Eq(3.12) the Lagrangian \mathcal{L}_S gives rise to a (S, H_S, N) ensemble where the generalized enthalpy is

$$H_S = E + V_{el} \quad (3.23)$$

where E is given by (3.43) and V_{el} by Eq(3.19).

A brief comparison between the traditional and new MD techniques is given in the following table.

Traditional MD	New MD
Constant cell volume	Variable cell shape and cell volume
Number of particles constant	Number of particles constant
Density constant, pressure varies with time	Pressure constant, density varies with time
Energy $E = \text{constant}$	Enthalpy $H = E + V_{el} = \text{constant}$
$3N$ variables	$3N+9$ variables

The additional 9 dynamical variables describe the time dependence of the shape of the MD cell. The change in shape of the MD cell is determined by difference between internal (kinetic + potential) stress tensor and the externally applied stress.

IV. A Static Study

(1). Brief Description of Potassium Chloride Crystal

Before going to study our main subject, the uniaxial applied stress (in addition to isotropic pressure) induced B1 to B2 transformation in KCl at zero temperature, it is convenient to give a short description of KCl crystal. This description would make our model of discussion clear. Some aspect of isotropic pressure induced transformation on our model will be discussed here.

It is an experimental fact that the alkali halides crystallize in the B1 structure in standard thermodynamic conditions, with the exception of cesium chloride, bromide and iodide, which crystallize in the B2 structure. Theoretically discussion of the relative stability between different structures shows that the actual structure is determined by the Gibbs free energy

$$G = U + PV - TS \quad (4.1)$$

the structure, which is thermodynamically the most stable, has the lowest free energy. At zero pressure and the absolute zero temperature a solid crystallizes in the structure with the lowest energy U.

The static energy per unit cell, $u=U/N$, is given by

$$u_{B1} = 6\Phi_{AH}(a/2) + 6\Phi_{AA}(\sqrt{2}a/2) + 6\Phi_{HH}(\sqrt{2}a/2) - 3.4952e^2/a \quad (4.2)$$

for the B1 structure, and

$$u_{B2} = 8\Phi_{AH}(\sqrt{3}a/2) + 3\Phi_{AA}(a) + 3\Phi_{HH}(a) + 6\Phi_{AA}(\sqrt{2}a) + 6\Phi_{HH}(\sqrt{2}a) - 2.0354e^2/a \quad (4.3)$$

for the B2 structure, where a is the corresponding lattice constant and e is the electronic charge. In our studies we use the parameterized Gordon-Kim potential^{[27], [67]} which takes following

forms:

$$\Phi_{AH} = \sum_{i=1}^4 C_{1i} \exp(-B_{1i}r)$$

$$\Phi_{AA} = \sum_{i=1}^4 C_{2i} \exp(-B_{2i}r)$$

(44)

$$\Phi_{HH} = \sum_{i=1}^4 C_{3i} \exp(-B_{3i}r)$$

the coefficient $\{C_{11}, \dots, C_{33}; B_{11}, \dots, B_{33}\}$ for KCl are as follows:

Table. (4.1)

ion pair	C_{j1}	C_{j2}	C_{j3}	C_{j4}
K^+Cl^- ; j=1	-44.35	97.07	-11.77	-0.316
K^+K^+ ; j=2	-828.4	3422.	-144.1	-18.81
Cl^-Cl^- ; j=3	-85.21	60.85	-7.061	-0.310

ion pair	B_{j1}	B_{j2}	B_{j3}	B_{j4}
K^+Cl^- ; j=1	1.557	1.460	1.220	0.937
K^+K^+ ; j=2	2.586	2.433	1.942	1.833
Cl^-Cl^- ; j=3	1.799	1.210	0.955	0.756

Here the atomic units with energy in Hartrees are used.

Using the potential (4.4), in writing (4.2) and (4.3) three more assumptions have been made: (a) The crystals are composed of the free ions; (b) The interactions of ions are pairwise additive; (c) The short-range interactions for B1 phase are restricted to first and second nearest neighbors, while in the B2 phase first-, second- and third-nearest-neighbors are considered.

Minimizing Eq(4.2) and Eq(4.3) with respect to lattice constant we got the equilibrium lattice constant and the static energy per unit cell for B1 and B2 structure at zero temperature and zero pressure respectively. The results are given in the table (4.2)

Table. (4.2)

	B1 structure	B2 structure
Lattice constant a	11.73a.u.=5.99Å	6.769a.u.=3.582Å
Lattice energy u	-.2875a.u. =-180.41Kcal/mole.	-.2855a.u. =-179.15Kcal/mole.

Note that the energy difference between two phases is 1.26 Kcal/mole, less than one percent of the lattice energy itself.

At 0°K the Gibbs free energies of two phases (per pair) are

$$G_{B1} = u_{B1}(r) + \frac{1}{4}r^3p \quad (4.5)$$

and

$$G_{B2} = u_{B2}(r') + r'^3p \quad (4.6)$$

where r and r' are the lattice constant in these phases.

A isotropic pressure induced phase transition is marked by the identity of the Gibbs free energy of the two phases:

$$G_{B1}(P_c) = G_{B2}(P_c) \quad (4.7)$$

This gives the pressure needed for triggering the transition, P_c , i.e., $P_c = 11.4$ Kbar; and $G_{B1}(P_c) = G_{B2}(P_c) = -171.68$ Kcal/mole. Comparing with $G_{B1}(P=0) = G_{B1}(a_{B1})$, this gives $\Delta G = G_{B1}(P_c) - G_{B1}(P=0) = 8.73$ Kcal/mole, which is approximately equal to the work to be done in order to trigger the transition. A schematical representation of the above discussions are given in the Fig. (4.1)

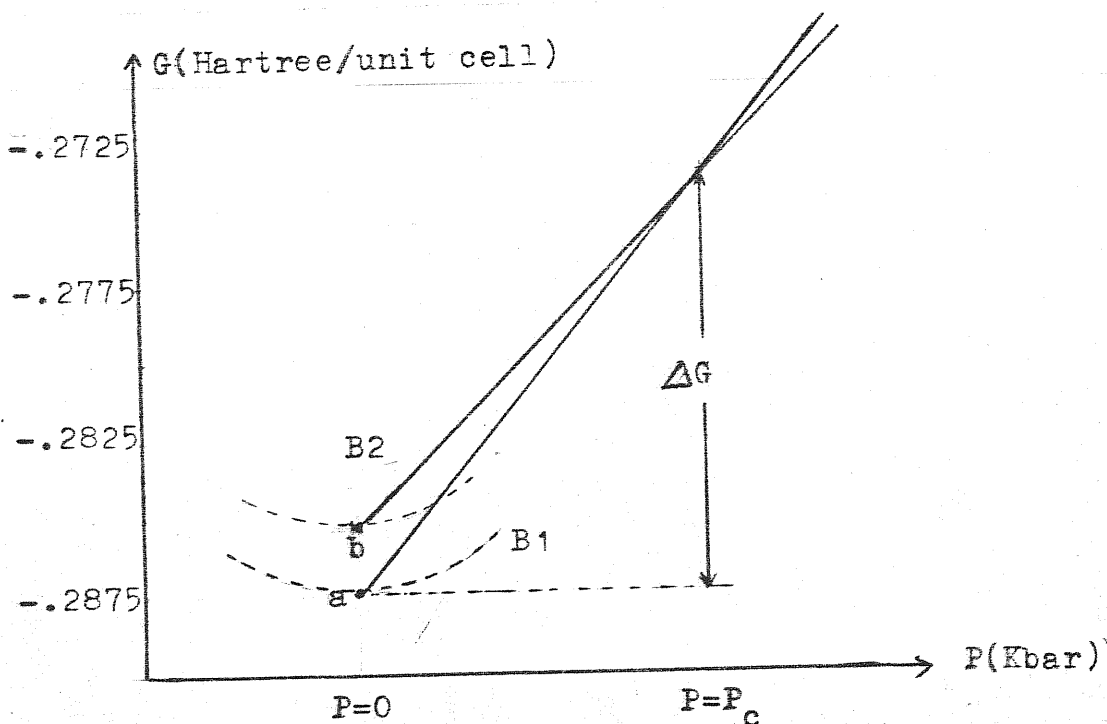


Fig. (4.1) A schematical representation of the pressure induced B1 to B2 transition; the points a and b indicate the local minimum energy for the B1 and B2 phases respectively.

At the transition point the lattice constant of KCl for the B1 and B2 structures are decreased to 5.91\AA and 3.543\AA respectively. Notice that the volume of the unit cell for B1 and B2 structure are $V_{B1} = \frac{1}{4}a_{B1}^3$ and $V_{B2} = a_{B2}^3$ respectively. This gives $\Delta V/V = 1\%$ approximately, i.e., the relative volume change of amount of 1% can be found in the transition.

The expression for the elastic constants can be obtained by comparing the long-wavelength limit of the dynamical matrix with the corresponding results from the elasticity theory⁽²²⁾. For the B1 structure this yields

$$C_{11} = -1.2780 \frac{e^2}{r_1^4} + \frac{1}{r_1} (\bar{\Phi}_{AH}'' + \bar{\Phi}_{HH}'' + \bar{\Phi}_{AA}'' + \frac{1}{r_2} (\bar{\Phi}'_{HH} + \bar{\Phi}'_{AA})), \quad (4.8)$$

$$C_{12} = 0.0565 \frac{e^2}{r_1^4} + \frac{1}{r_1} \left(-\frac{1}{r_1} \bar{\Phi}'_{AH} + \frac{1}{2} (\bar{\Phi}''_{HH} + \bar{\Phi}''_{AA}) - \frac{5}{2r_2} (\bar{\Phi}'_{HH} + \bar{\Phi}'_{AA}) \right) \quad (4.9)$$

$$C_{44} = 0.6390 \frac{e^2}{r_1^4} + \frac{1}{r_1} \left(-\frac{1}{r_1} \bar{\Phi}'_{AH} + \frac{1}{2} (\bar{\Phi}''_{HH} + \bar{\Phi}''_{AA}) + \frac{3}{2r_2} (\bar{\Phi}'_{HH} + \bar{\Phi}'_{AA}) \right) \quad (4.10)$$

where the derivatives of the $\bar{\Phi}_{AH}$ potential are evaluated at $r_1 = \frac{1}{2}a$, and the derivatives of $\bar{\Phi}_{AA}$ and $\bar{\Phi}_{HH}$ at $r_2 = \sqrt{2}a/2$. Since the expressions give the elastic behavior of the static lattice as a function of lattice constant we shall refer to them as a static elastic constants.

This gives :

$$C_{11} = 5.714; \quad C_{12} = 0.8914; \quad C_{44} = 0.8914. \quad (4.11)$$

in the units of 10^{11} dynes/cm². Note that the relation of $C_{12} = C_{44}$ is satisfied.

Table.(4.3) gives some experimental data for the KCl crystal at room temperature and at atmospheric pressure.

Table. (4.3)

	A	K	W_{vib}	C_v	P_c
unit	Å	$10^{-12} \text{cm}^2 \text{dyne}^{-1}$	10^{-12}erg	10^{-16}erg	Kbar
value	6.294	5.73	0.254	8.04	12
	$-\frac{1}{K} \left(\frac{\partial K}{\partial P} \right)_T$	$\frac{T}{C_v} \left(\frac{\partial C}{\partial T} \right)_v$	$\frac{1}{K} \left(\frac{\partial K}{\partial T} \right)_P$	D_e	
unit	$10^{-12} \text{cm}^2 \text{dyne}^{-1}$		10^{-4}deg^{-1}	Kcal/mole	
value	30	0.0574	3.5	165.8	

here A is the lattice constant ;
 C_v is the heat capacity at constant volume ; (The coefficient of volum thermal expansion equals to $11.01 \times 10^{-4} \text{deg}^{-1}$.)
 W_{vib} is the vibrational energy ;
 K is the isothermal compressibility ;
 P_c is the transition pressure ;
 D_e is the cohesive energy at room temperature. (The cohesive energy at 0°K is 169.5 Kcal/mole) .

All these data are taken from Ref.(8) .

(2). Potassium Chloride Crystal under uniaxial tensile loading.

Recently Parrinello and Rahman⁽³⁸⁾ have presented a microscopic mechanism of KCl transforming from the B1 to the B2 structure, as described in section 2 . The process of the transformation consists of two steps. During the first step the B1 (fcc) lattice continuously modifies its configuration and finally reaches a deformed fct lattice characterized by parameters $\lambda_2 = 1.2247\lambda_1$, $\cos \varphi = 0.3333$, i.e., $\varphi = 70.53^\circ$. The second step completed by a collective ion jumps ; i.e., ions of alternate planes in the (100) direction collectively jump along the (0,-1,1) direction. The jump can be described by a translation vector $(0, -\frac{1}{2}, \frac{1}{2}) a \frac{\sqrt{2}}{2}$.

Note that the discontinuous way of ion move may mean that at the end of the first step system reaches a instable point.

This mechanism would stimulate us to think that the configuration at the end of the first step can be obtained by applying a external uniaxial tensile loading along (0,1,1) direction, compannying a suppression on (1,0,0) direction. And this instability may be characterized by softening of a transverse acoustic, (1,0,0), zone boundary phonon with polarization vector in the (0,-1,1) direction, as pointed out by Parrinello and Rahman⁽³⁸⁾.

Based on the above consideration the main aims of our static study are as follows: Starting from the B1 equilibrium configuration, i.e., perfect fcc lattice with lattice constant $a=5.99\text{\AA}$, we apply a uniaxial stress along (0,1,1) direction to the KCl crystal to see how the system modifies its configuration to reach a instable point; In addition we apply a isotropic pressure and to investigate what is the role of this additionally applied pressure. As a preliminary study, the effects of the harmonic vibrations are neglected. this study will then be naturally extended to including the harmonic vibrations at zero and finite temperatures.

(A). Formulation.

If we assume that the vibrational energy levels of the system are those of independent harmonic oscillators with frequencies ν_i , then the free energy per unit cell is taken the simple form²²:

$$F = u + \frac{1}{2} \frac{1}{N} \sum_i h \nu_i + \frac{1}{N} KT \sum_i \ln(1 - \exp(-h\nu_i/KT)) \quad (4.12)_1$$

where T is the temperature, h is Plank's constant and K is Boltman's constant. The Gibbs free energy per unit cell is

$$G = F + V_{el} \quad (4.12)_2$$

where V_{el} is the elastic energy per unit cell. From now on we will neglect harmonic vibrations. In this case the free energy F is simply the static lattice energy per unit cell.

When a general external stress applied, the Gibbs free energy will be a function of the configurational parameters as well as the external stress. Let us apply a uniaxial stress S along (0,1,1) direction in addition to a isotropic preture P, the Gibbs free energy per unit cell can be expressed as a function of the configurational parameters $\{\tau_1, \tau_2, \text{and } \cos\varphi\}$ for a given lattice

constant a .

$$G = V_s(\pi_1, \pi_2, \cos\varphi; a) - \frac{\alpha(\pi_1, \pi_2, \cos\varphi)}{a} + V_{el} \quad (4.13)$$

where V_s is the short range part of the static energy and is given by

$$V_s = 2\Phi_{AH}(\pi_1 \frac{a}{2}) + 4\Phi_{AH}(\pi_2 \frac{a}{2}) + \Phi_{AA}(\pi_2 a \cos \frac{\varphi}{2}) + \Phi_{AA}(\pi_2 a \sin \frac{\varphi}{2}) + 4\Phi_{AA}(\frac{1}{2}\sqrt{\pi_1^2 + \pi_2^2} a) + \Phi_{HH}(\pi_2 a \cos \frac{\varphi}{2}) + \Phi_{HH}(\pi_2 a \sin \frac{\varphi}{2}) + 4\Phi_{HH}(\frac{1}{2}\sqrt{\pi_1^2 + \pi_2^2} a) \quad (4.14)$$

The second term in rhs of Eq(4.13) is Madlung energy per unit cell; where the $\alpha(\pi_1, \pi_2, \cos\varphi)$ is Madlung constant for the configuration $\{\pi_1, \pi_2, \cos\varphi\}$ with respect to a and we used Eward method (68)(69) to express $\alpha(\pi_1, \pi_2, \cos\varphi)$ as follows:

$$\alpha(\pi_1, \pi_2, \cos\varphi) = 2\left(\frac{\eta}{\pi}\right)^{\frac{1}{2}} + \sum_{l_1, l_2, l_3} (-1)^{l_1+l_2+l_3} R(l_1, l_2, l_3)^{-1} F(\eta^{\frac{1}{2}} R(l_1, l_2, l_3)) - \frac{\varepsilon}{\pi_1 \pi \sin\varphi} \sum_{m_1, m_2, m_3}' G(m_1, m_2, m_3)^{-1} \exp\left(-\frac{\pi^2}{\pi_2^2 \eta} G(m_1, m_2, m_3)\right) \quad (4.15)$$

where

$$G(m_1, m_2, m_3) = \left(\frac{\pi_2}{\pi_1}\right)^2 (-m_1 + m_2 + m_3)^2 + \frac{m_1^2}{[\cos \frac{1}{2}\varphi]^2} + \frac{(-m_2 + m_3)^2}{(\sin \frac{1}{2}\varphi)^2} \quad (4.16)$$

$$R(l_1, l_2, l_3) = \frac{1}{2} (l_1^2 \pi_1^2 + \pi_2^2 (l_2^2 + l_3^2 + 2l_2 l_3 \cos\varphi))^{\frac{1}{2}} \quad (4.17)$$

and

$$F(x) = \frac{2}{\sqrt{\pi}} \int_x^{\infty} \exp(-s^2) ds \quad (4.18)$$

is a complementary error function. Here η is a dimensionless parameter, whose value can be chosen so as to ensure quick convergence. The prime in the sum of m_1, m_2, m_3 indicates that sum runs over those integers that $m_1 + m_2 + m_3 = \text{odd integers}$. Sum over l_1, l_2, l_3 runs over all integers with the exception for l_1, l_2, l_3 simultaneously take zero values.

The elastic energy per unit cell V_{el} in Eq(4.13) is now given by

$$V_{el} = \Omega_0 (S_{22} (\cos^2 \frac{1}{2}\varphi \pi_2^2 - 0.5) + F(\pi_1 \pi_2^2 \sin\varphi - 1)) \quad (4.19)$$

Now the volume of unit cell of undistorted and distorted configurations are

$$\Omega_0 = \frac{1}{4} a^3 \quad (4.20)_1$$

$$\Omega = \frac{1}{4} \pi_1 \pi_2 \sin \varphi a^3 \quad (4.20)_2$$

The strain tensor $\underline{\epsilon}$ is given by

$$\underline{\epsilon} = \begin{pmatrix} \frac{\lambda_1^2 - 1}{2} & 0 & 0 \\ 0 & \frac{\lambda_2^2 - 1}{2} & \lambda_2 (\cos^2 \frac{\varphi}{2} - \frac{1}{2}) \\ 0 & \lambda_2 (\cos^2 \frac{\varphi}{2} - \frac{1}{2}) & \frac{\lambda_2^2 - 1}{2} \end{pmatrix} \quad (4.21)$$

The external stress tensor \underline{S} is

$$\underline{S} = \begin{pmatrix} 0 & 0 & 0 \\ 0 & \frac{1}{2} S_{22} & \frac{1}{2} S_{22} \\ 0 & \frac{1}{2} S_{22} & \frac{1}{2} S_{22} \end{pmatrix} \quad (4.22)$$

The Eq (4.19) can be obtained by substituting Eq.(4.20), (4.21) and (4.22) into the Eq.(4.19).

For a fixed externally applied stress, we minimize the G in Eq(4.13) with respect to the configuration parameters $\{\pi_1, \pi_2$ and $\cos \varphi\}$, we get the configuration characterized by $\{\bar{\pi}_1, \bar{\pi}_2, \cos \bar{\varphi}\}$ and local minimum Gibbs free energy. Then the configuration $\{\bar{\pi}_1, \bar{\pi}_2, \cos \bar{\varphi}\}$ is the relative stable configuration under the corresponding external stress. Substituting the configuration parameters $\{\bar{\pi}_1, \bar{\pi}_2, \cos \bar{\varphi}\}$ into the free energy (now is the lattice energy) expression,

$$F = V_s(\bar{\pi}_1, \bar{\pi}_2, \cos \bar{\varphi}) - \frac{\alpha(\bar{\pi}_1, \bar{\pi}_2, \cos \bar{\varphi})}{a} \quad (4.23)$$

we get the corresponding free energy. Changing the external stress step by step, repeat the above procedures we can follow the path in which the system evolves its configurations.

In order to monitor the instability of each configuration generated, we set up a dynamical matrix depending on the configuration parameters $\{\bar{\pi}_1, \bar{\pi}_2, \cos \bar{\varphi}\}$. The general expression for the dynamical matrix of an ionic crystal with pairwise short range forces are given in Maradudin et.al.^[70] Diagonalizing the dynamical matrix for a wave vector q , we get the phonon frequencies for that q .

We will take following equation

$$W_k^2 > 0 \quad (k=1, \dots, 3N) \quad (4.24)$$

as the microscopic stability condition. a purely imaginary frequency of vibrations implies that a normal mode of vibration would grow exponentially either in the past or in the future, and the solid subject to a small displacement, would disrupt exponentially with time instead of executing small vibrations around the equilibrium configurations.

(B). Numerical method and results.

Obviously minimizing Eq.(4.13) can not be done analytically. Our numerical method is simply evaluate Eq.(4.13) for a sufficiently large number of configurations specified by parameters $\{\lambda_1, \lambda_2, \cos\theta\}$ for each externally applied stress. These configurations can be carefully chosen around a center configuration which can be predicted by elastic theory for small stress or can be estimated by the last step of calculation. Then for each configuration we get a value of G; Among those values the lowest one can be taken as minimum of G approximately. Obviously the accuracy depends on that how fine the mesh of the configuration space will be.

Our procedures are as follows: Applying tensile uniaxial loading along (0,1,1) direction described in Eq(4.22), in addition to a certain isotropic pressure P. First we fixed the value of P, then raised the tensile load from 0 to S_{22max} through a series of small intermediate steps at $S_{22} = \Delta S_{22}, 2\Delta S_{22}, \dots$. In this calculation $\Delta S_{22} = 2.94 \text{Kbar}$. Here S_{22max} is the value of S_{22} , under this value of applied external stress distorted lattice becomes instable. Repeating above procedures for each value of S_{22} we can follow the path in which the system modifies its configuration to reach a instable point. In order to looking for the roles of the additionally applied isotropic pressure, for each value of P we repeated the above procedures. In the present work the input data of P are $P = 0, 12 \text{Kbar}$ and 44Kbar respectively.

The results are summarized in tables (4.4)-(4.9).

Table. (4.4)

Isotropic pressure P=0.

S22	α_1	α_2	COS ϕ	EMAD	EV	E
0.000000	1.0000	1.0000	0.0000	-.308447	.020986	-.287460
-.000010	.9992	1.0025	-.0160	-.308002	.020560	-.287441
-.000020	.9983	1.0051	.0330	-.307518	.020137	-.287382
-.000030	.9970	1.0085	.0530	-.306871	.019615	-.287256
-.000040	.9956	1.0115	.0700	-.306304	.019201	-.287103
-.000050	.9940	1.0155	.0880	-.305532	.018650	-.286881
-.000060	.9920	1.0200	.1100	-.304639	.018088	-.286551
-.000070	.9898	1.0250	.1300	-.303676	.017511	-.286165
-.000080	.9876	1.0305	.1480	-.302641	.016911	-.285730
-.000090	.9848	1.0370	.1700	-.301424	.016294	-.285130
-.000100	.9812	1.0455	.1940	-.299923	.015599	-.284324
-.000110	.9768	1.0565	.2240	-.297997	.014841	-.283155
-.000120	.9713	1.0716	.2540	-.295651	.014048	-.281603
-.000130	.9624	1.0988	.2980	-.291916	.013224	-.278692
-.000131	.9608	1.1050	.3060	-.291127	.013088	-.278039
-.000132	.9576	1.1162	.3200	-.289827	.012982	-.276844

Table. (4.5)

Isotropic pressure P=12 Kbar.

S22	α_1	α_2	COS ϕ	EMAD	EV	E
0.000000	1.0000	1.0000	0.0000	-.312934	.025776	-.287158
-.000010	.9994	1.0018	-.0160	-.312607	.025423	-.287184
-.000020	.9986	1.0044	.0360	-.312113	.024941	-.287171
-.000030	.9976	1.0066	.0560	-.311636	.024536	-.287100
-.000040	.9964	1.0096	.0760	-.310999	.024016	-.286984
-.000050	.9950	1.0126	.0960	-.310347	.023538	-.286808
-.000060	.9935	1.0160	.1120	-.309635	.023005	-.286630
-.000070	.9916	1.0200	.1360	-.308733	.022447	-.286266
-.000080	.9896	1.0244	.1560	-.307784	.021855	-.285928
-.000090	.9874	1.0294	.1760	-.306727	.021228	-.285499
-.000100	.9846	1.0356	.2000	-.305419	.020532	-.284887
-.000110	.9820	1.0420	.2200	-.304137	.019862	-.284275
-.000120	.9786	1.0500	.2440	-.302582	.019157	-.283425
-.000130	.9744	1.0604	.2720	-.300642	.018384	-.282257

Table. (4.6)

Isotropic pressure P=44 Kbar.

S22	α_1	α_2	COS ϕ	EMAD	EV	E
0.000000	1.0000	1.0000	0.0000	-.322091	.037567	-.284524
-.000010	.9994	1.0016	-.0240	-.321777	.037165	-.284612
-.000020	.9988	1.0032	.0460	-.321403	.036767	-.284637
-.000030	.9980	1.0048	.0700	-.320976	.036403	-.284573
-.000040	.9972	1.0070	.0940	-.320354	.035868	-.284486
-.000050	.9960	1.0096	.1160	-.319657	.035297	-.284360
-.000060	.9946	1.0122	.1400	-.318894	.034774	-.284121
-.000070	.9932	1.0154	.1620	-.317989	.034110	-.283879
-.000080	.9916	1.0186	.1820	-.317104	.033511	-.283594
-.000085	.9908	1.0202	.1940	-.316597	.033219	-.283378

Table. (4.7)

Isotropic pressure P=0.

-S22	Ta1 (0,-1,1)	Ta2 (0,1,1)	La (1,0,0)	To1 (0,-1,1)	To2 (0,1,1)	Lo (1,0,0)
0.00000	1.3756	1.3756	3.3000	3.1390	3.1390	3.0759
0.00001	1.3726	1.4049	3.3260	3.0617	3.1076	3.0794
0.00002	1.2959	1.4457	3.3381	2.9862	3.0796	3.0748
0.00003	1.2522	1.4935	3.3564	2.8934	3.0388	3.0684
0.00004	1.2135	1.5337	3.3779	2.8146	3.0012	3.0623
0.00005	1.1726	1.5771	3.4018	2.7187	2.9438	3.0535
0.00006	1.1194	1.6292	3.4330	2.6109	2.8804	3.0427
0.00007	1.0694	1.6772	3.4683	2.5013	2.8036	3.0299
0.00008	1.0232	1.7212	3.5075	2.3896	2.7177	3.0150
0.00009	0.9618	1.7739	3.5502	2.2622	2.6077	2.9962
0.00010	0.8892	1.8318	3.6122	2.1088	2.4640	2.9701
0.00011	0.7870	1.9019	3.6880	1.9233	2.2769	2.9346
0.00012	0.6682	1.9787	3.7882	1.6981	2.0477	2.8827
0.00013	0.4281	2.0979	3.9557	1.3477	1.4842	2.7879
0.000131	0.3716	2.1171	3.9856	1.2703	1.3619	2.7609
0.000132	0.2269	2.1502	4.0486	1.1302	1.1434	2.7187

Table. (4.8)

Isotropic pressure P=12 Kbar.

-S22	Ta1	Ta2	La	To1	To2	Lo
0.00000	1.3185	1.3185	3.6369	3.4425	3.4425	3.0958
0.00001	1.2802	1.3588	3.6463	3.3785	3.4323	3.0928
0.00002	1.2313	1.4087	3.6625	3.2926	3.4114	3.0883
0.00003	1.1805	1.4576	3.6748	3.2160	3.3975	3.0846
0.00004	1.1284	1.5068	3.6941	3.1256	3.3658	3.0792
0.00005	1.0733	1.5552	3.7174	3.0372	3.3332	3.0734
0.00006	1.0285	1.5950	3.7406	2.9500	3.2854	3.0665
0.00007	0.9546	1.6524	3.7748	2.8417	3.2356	3.0579
0.00008	0.8892	1.7010	3.8092	2.7360	3.1707	3.0483
0.00009	0.8183	1.7500	3.8472	2.6274	3.0926	3.0362
0.00010	0.7221	1.8087	3.8965	2.4909	2.9938	3.0206
0.00011	0.6312	1.8576	3.9425	2.3660	2.8855	3.0035
0.00012	0.4949	1.9161	4.0046	2.2185	2.7489	2.9810
0.00013	0.2480	1.9835	4.0826	2.0417	2.5684	2.9806

Table. (4.9)

Isotropic pressure P=44 Kbar.

-S22	Ta1	Ta2	La	To1	To2	Lo
0.00000	1.173	1.173	4.330	4.085	4.085	3.069
0.00001	1.097	1.243	4.340	3.998	4.101	3.068
0.00002	1.024	1.305	4.351	3.916	4.111	3.068
0.00003	0.978	1.371	4.379	3.829	4.124	3.068
0.00004	0.845	1.437	4.379	3.732	4.121	3.067
0.00005	0.751	1.496	4.400	3.632	4.105	3.066
0.00006	0.628	1.558	4.426	3.529	4.091	3.064
0.00007	0.494	1.616	4.451	3.422	4.058	3.062
0.00008	0.321	1.668	4.480	3.321	4.021	3.060
0.000085	0.137	1.698	4.495	3.267	4.005	3.058

The units in table (4.4)-(4.9) are as follows :

1. Energy in unit of Hartree per cell.
2. Frequency in unit of 10^{13} Hz.
3. Stress in unit of $0.2942 \cdot 10^6$ Kbar.

The notations used in tables (4.4)--(4.6) are as follows: S_{22} is the external stress along (011) direction; $\lambda_i, \mu_i, \cos\varphi$ as usual are configurational parameters with reference to the reference state. At $P=0$, as mentioned before, the reference state is the perfect fcc lattice with lattice constant $a=11.33a.u.$; When the only hydrostatic pressure $P, P \neq 0$, applied, the crystal is forced into contracting, but maintains a perfect fcc lattice, i.e., a fcc lattice with shorter lattice constant. In the cases of $P_1=12\text{Kbar}$ and $P_2=44\text{Kbar}$ the lattice constant decreases to $a_1=11.168 a.u.$ and $a_2=10.851 a.u.$ respectively. In the cases of $P \neq 0$, we take this contracted perfect fcc lattice as a reference state. EMAD is Madlung energy; EV is the short range part energy. E is the free energy (now is lattice energy), i.e., sum of EMAD and EV. Each row in the table corresponds to one configuration. The configuration in the last row is very close to the instable point. From the table (4.4)--(4.6) we can see how the configuration and lattice energy vary with the external stress.

The tables (4.7)--(4.9) show how the frequencies of the various branches of (1,0,0) zone boundary phonon vary with the external stress. The titles of the six columns, i.e. Ta, La, To and LO, mean the frequencies of transverse acoustic, longitudinal acoustic, transverse optical and longitudinal optical modes respectively. The polarization vectors are indicated under the each title. Note that the frequency of a transverse acoustic mode with polarization vector in (0,-1,1) direction at the last row of each table is very close to zero.

(C). Conclusions.

From the numerical results we come to the conclusions that:

a). The numerical results agree with the elastic theory in the linear strain-stress relation for small stress. In the case of small stress, knowing the external stress and the elastic constant C_{11}, C_{12} and C_{44} we can evaluate the correspondent strains by the elastic theory⁶⁹:

$$\bar{\epsilon}_{yy} = \frac{1}{2} S_{22} / (C_{11} + C_{12} - 2C_{12}^2 / C_{11}) \quad (4.25)$$

$$\bar{\epsilon}_{xx} = -C_{12} \bar{\epsilon}_{yy} / C_{11} \quad (4.26)$$

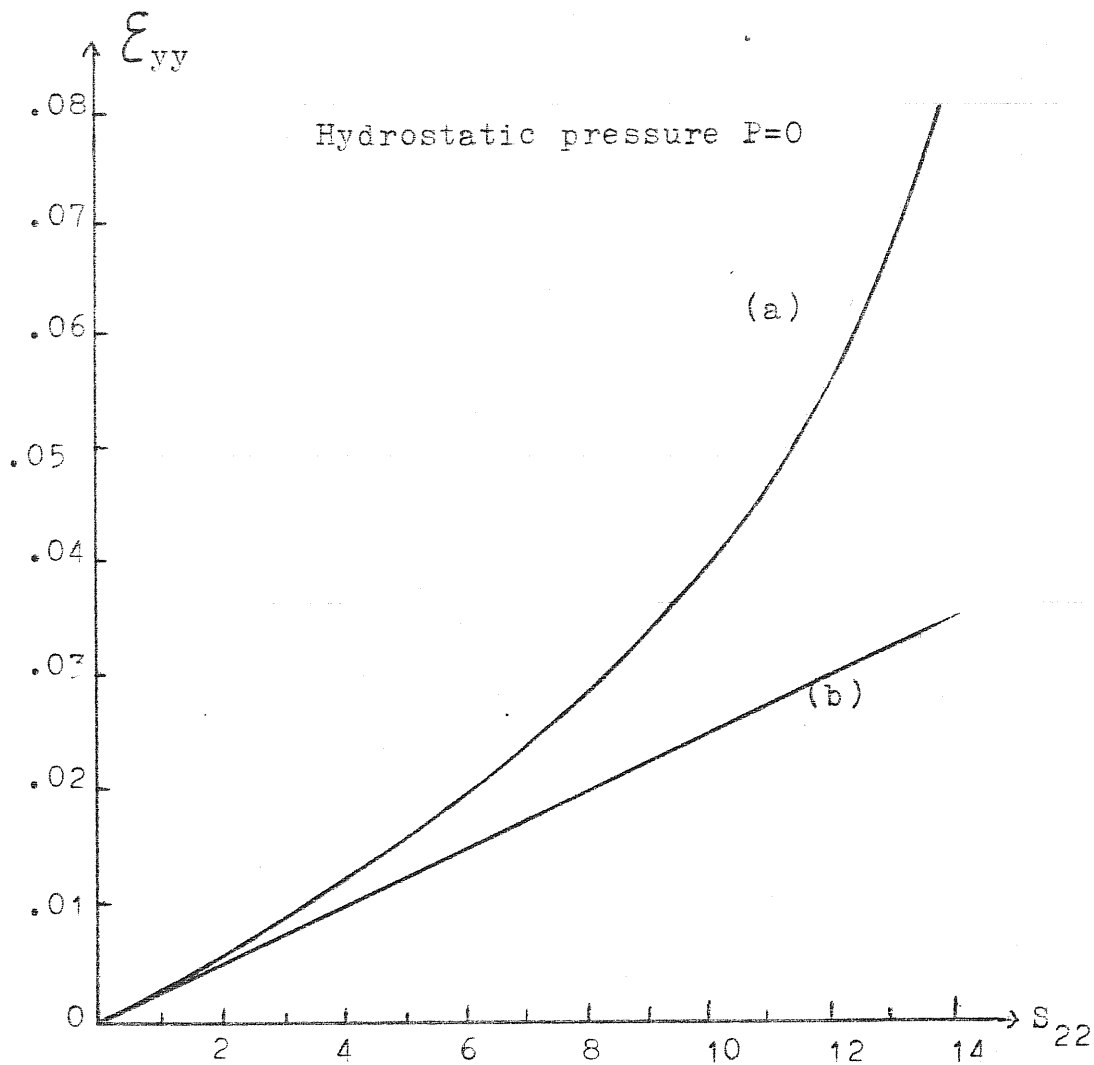


Fig. (4.2) A comparison numerical results with the elastic theory. the curve (a) and (b) are the plots of table (4.4) and the Eq (4.25) respectively. Here S_{22} is in unit of 2.94Kbar.

and

$$\cos \bar{\varphi} = \frac{1}{2} S_{22} / (C_{44} \pi_1 \pi_2) \quad (4.27)$$

On the other hand from the our results we can get strains as follows:

$$\epsilon_{yy} = \pi_2 - 1 \quad (4.28)$$

and

$$\epsilon_{xx} = \pi_1 - 1$$

The table (4.10) will give numerical comparison for some small stress.

Here the values of C_{11} , C_{12} and C_{44} in Eq (4.25)-(4.27) are given by Eq. (4.11).

Table. (4.10)

S_{22}	ϵ_{yy}	$\bar{\epsilon}_{yy}$	ϵ_{xx}	$\bar{\epsilon}_{xx}$	$\cos\varphi$	$\cos\bar{\varphi}$
1	.0025	.0027	.0008	.00077	.016	.016
2	.0051	.0047	.0017	.0015	.033	.033
3	.0085	.0070	.0030	.0022	.053	.050
4.	.0115	.0097	.0044	.0029	.070	.065

As the external stress increases the deviation from the linear relation become larger and larger, and finally blow up with the slightly increasing the stress. The system is going to reach a instable point.

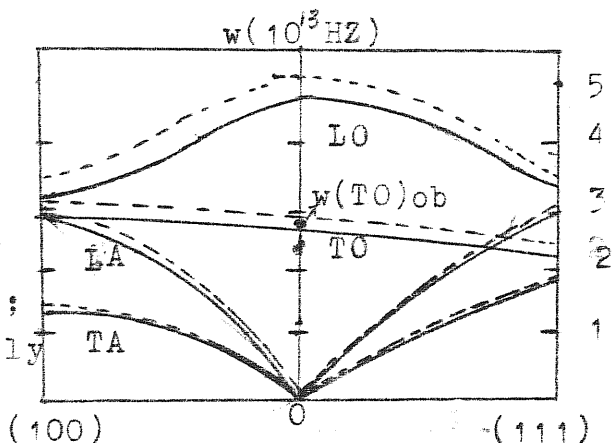
b). Comparising the last rows of table (4.4)-(4.6), one can find that the higher additionally applied hydrostatic pressure the less S_{22max} system needed to trigger the transition. Moreover the pressure would suppress the free energy barrier, we will denote it as ΔE . A comparison is given in the table (4.11).

Table .(4.11)

P (Kbar)	S_{22max} (2.94Kbar)	ΔE (Kcal/mole)
0	≈ 13.2	6.69
12	≈ 13	3.26
44	≈ 8.5	2.56

c). A discussion on phonon behaviours:

Fig.(4.7) Phonon dispersion curves for KCl. The real curves by Hardy⁽⁷¹⁾, derived for rigid ions, at $T=80^\circ K$. The dot lines from our result by using the parameterized Gordon-Kim potential; The " $w(TO)_{ob}$ " means experimentally observed value.



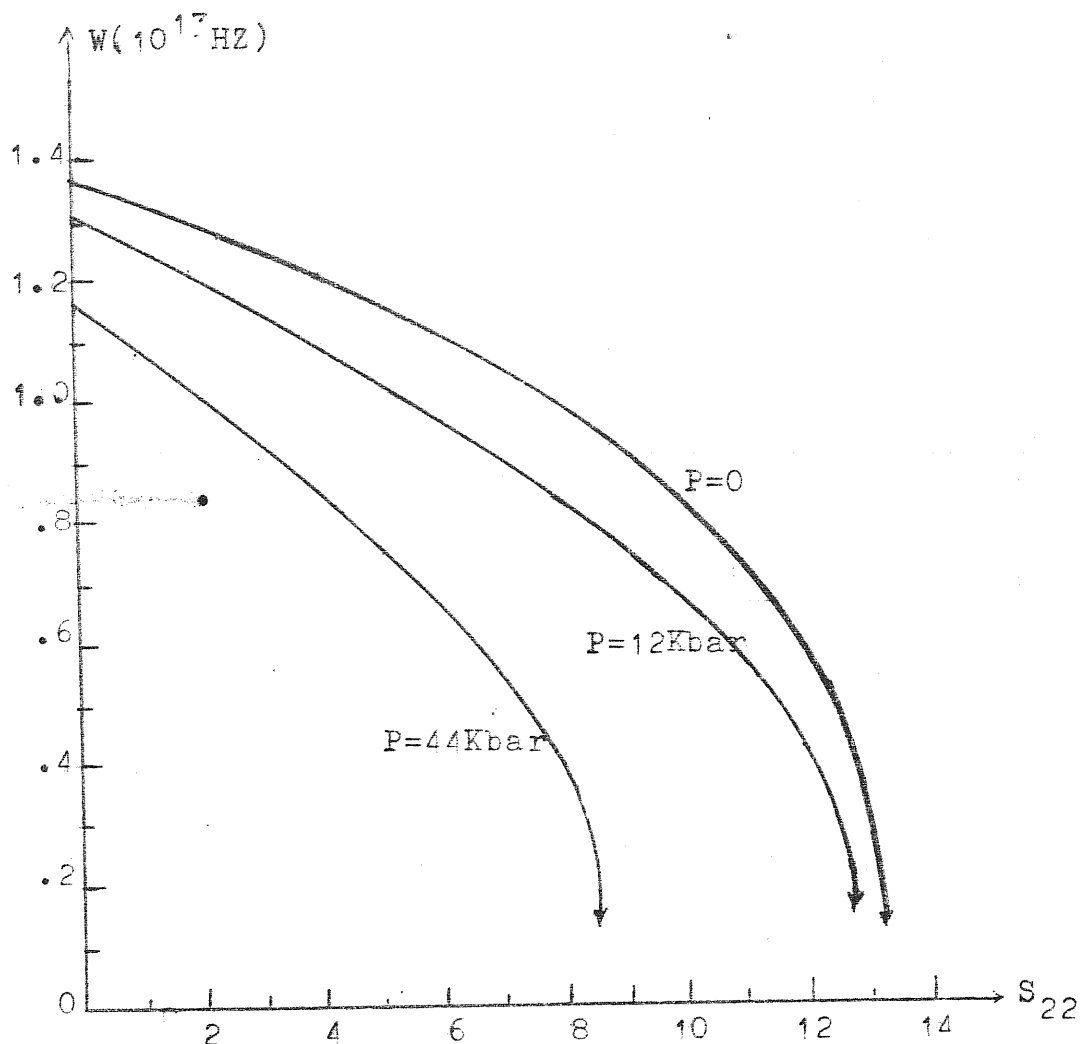


Fig.(4.4) The frequency of a transverse acoustic, $(1,0,0)$, zone boundary phonon with polarization vector in the $(0,-1,1)$ direction decreases with the increase of the external stress. And the S_{22max} depends on the additionally applied hydrostatic pressure; the larger pressure, the less S_{22max} .

As mentioned before that the phonon frequencies depend on the configuration parameters $n_1, n_2, \cos \varphi$, when a general stress is applied (of course depend on the lattice constant). In the case of $P=0$ and $S_{22}=0$, i.e., $n_1=1, n_2=1, \cos \varphi=0$ and lattice constant $a=11.33$ a.u., we get the phonon dispersion curves for KCl, as shown in Fig.(4.7). Note that the transverse branches are degenerated and it is so when only hydrostatic pressure is applied.

When an external tensile loading applies along $(0,1,1)$ direction the degenerated transvers acoustic and optical branch each split into two: one with polarization vector in $(0,1,1)$ direction (i.e., Ta_2 and To_2); the other with polarization vector in $(0,-1,1)$ direction (i.e., Ta_1 and To_1). We are interested in that how the frequencies of the various branches of $(1,0,0)$ zone boundary phonon vary with the external stress.

From table (4.7)-(4.9) one can see that Lo and La are not sensitive to the external stress. The To_1 and To_2 decrease monotonously with increasing the external stress; Ta_2 grow up with increasing the external stress. Among all these the Ta_1 is lowest. When the external stress increases Ta_1 drop down almost linearly at first; as the stress increases up to certain value and after that Ta_1 drops down steeply to reach the instable point, which depends on the additionally applied hydrostatic pressures.

d). It should be noticed here that:

i). At the case of $P=0$, i.e., a pure uniaxial external loading applies to the crystal, as S_{22} increases to S_{22max} Ta_1 becomes imaginary, it means the system becomes microscopically instable. As mentioned before at $S_{22}=S_{22max}$ the strain ϵ_{yy} blows up steeply with slightly increasing the external stress, it may mean the system also becomes elastically instable.

ii). At the cases of $P \neq 0$, e.g., the case of $P=44\text{Kbar}$, when system becomes microscopically instable and may still be elastically stable, as one can see from the last row of table (4.9), at $S_{22}=S_{22max}$ the deviation of the system from the linear strain-stress relation is not very far.

We may come to the conclusion that for a real transformation it is necessary to apply the hydrostatic pressure, but externally applied stress or locally induced stress may trigger the transformation.

In order to extend our study to including the effects of harmonic vibrations we attempt to use the "many point scheme" for evaluating the BZ sum in Eq(4.12). A brief discussion will be given in the next subsection.

(7). Baldereschi Point and Many Points Scheme for Evaluating Brillouin Zone Sum

The determination of many physical properties of crystal (e.g, the total energy of the crystal, the charge density, etc) often requires integrations of periodic functions over the Brillouin Zone (B.Z.). Ordinarily, the periodic functions does not have a simple analytic form, the evaluation of the integrant for a great number of points in the B.Z. is very complicated and time consuming. Previously, various approximate methods⁽⁷⁰⁾ have been used to obtain these functional values throughout the B.Z. by interpolation schemes which require a knowledge of the functional values at a finite number of points. Recently an alternative method was proposed in which only a single " Baldereschi mean value point"⁽⁷³⁾⁽⁷⁴⁾ or a few careffully chosen special points⁽⁷⁵⁾⁽⁷⁶⁾ in the B.Z. are used in order to give a good approximation. The Baldereschi point and the many special points for the cubic lattices have been generated⁽⁷³⁾⁽⁷⁵⁾, for some non cubic lattices have been presented⁽⁷⁷⁾⁽⁷⁸⁾. We will discuss the central idea of this method and present the special points of the tetragonal face-centered (f.c.t) lattice and deformed f.c.t lattice based on our calculation.

(A). The Many Special Point Scheme.

Let us denote some periodic function by $f(\vec{k})$, which can be expanded in a Fourier series :

$$f(\vec{k}) = f_0 + \sum_{m=1}^{\infty} f_m A_m(\vec{k}) \quad (4.29)$$

where

$$A_m(\vec{k}) = \sum_{|\vec{R}_m|=d_m} \exp(i\vec{k} \cdot \vec{R}_m) ; m=1, 2, \dots \quad (4.29)$$

d_m is the m -th nearest-neighbor distance and $d_m < d_{m+1}$. We have

$$\int_{B.Z} A_m(\vec{k}) d\vec{k} = 0 \quad (4.30)$$

f_m usually drops rapidly in magnitude as m increases.

Integration of $f(\vec{k})$ over the B.Z. gives

$$\begin{aligned} I &= \frac{\Omega}{(2\pi)^3} \int_{B.Z} f(\vec{k}) d\vec{k} \\ &= f_0 + \frac{\Omega}{(2\pi)^3} \sum_{m=1}^{\infty} f_m \int_{B.Z} A_m(\vec{k}) d\vec{k} = f_0 \quad (4.31) \end{aligned}$$

On the other hand, we also have

$$f_0 = f(\vec{k}_i) - \sum_{m=1}^{\infty} f_m A_m(\vec{k}_i) \quad (4.32)$$

Thus

$$f_0 = f(\vec{k}_i) \quad (4.33)$$

provided

$$A_m(\vec{k}_i) = 0 \quad \text{for } m=1, 2, \dots, \infty \quad (4.34)$$

Baldereschi⁽⁷⁴⁾ first obtained a "mean value point", \vec{k}_0 , which obeys Eq (4.34) for $m=1, 2, 3$. This point gives $I = f(\vec{k}_0)$ if f_m becomes very small for $m > 4$.

In order to obtain a better approximation to the integral, a many-point scheme⁽⁷⁵⁾ becomes necessary. If \vec{k}_1 and \vec{k}_2 are the points which satisfy $A_s(\vec{k}_1) = 0$ for $s = s_1, s_2, \dots$ and $A_t(\vec{k}_2) = 0$ for $t = t_1, t_2, \dots$, then the set of points \vec{g}_i , which are generated from \vec{k}_1 and \vec{k}_2 using the following relation:

$$\vec{g}_i = \vec{k}_1 + T_i \vec{k}_2 \quad (4.35)$$

will satisfy

$$\sum_{i=1}^n \alpha_i A_m(\vec{g}_i) = 0 \quad \text{for } m = s_1, s_2, \dots, t_1, t_2, \dots \quad (4.36)$$

Here the T_i range over all the operations of the lattice point group of order N . Some of the \vec{g}_i so generated are related to each other by one of the symmetry operations T_i . We group these points together, give a weighting factor α_i to the group and sum over only those \vec{g}_i 's which are not related by T_i . Therefore, $n \leq N$ in Eq(4.36). After this set of points is obtained the integral in Eq(4.31) may be written as

$$I = f_0 = \sum_{i=1}^n \alpha_i f(\vec{g}_i) - \sum_m f_m \sum_i \alpha_i A_m(\vec{g}_i) \quad (4.37)$$

In the many point approximationⁱ, we ignore the second term in Eq(4.37), i.e.

$$I = f_0 = \sum_{i=1}^n \alpha_i f(\vec{g}_i) \quad (4.38)$$

Note that

$$\sum_{i=1}^n \alpha_i = 1 \quad (4.39)$$

This becomes an excellent approximation if Eq(4.36) is

satisfied for m covering a large number of neighbours. In cases where an even higher degree of accuracy is sought, one may repeat the above procedure in order to generate a new set of points \bar{g}_i which satisfies Eq(4.36) for more value of m . The new set of points is obtained by choosing a point \bar{k}_3 which satisfies $A_r(\bar{k}_3) = 0$ for $r=r_1, r_2, \dots$ and the r includes some value different from s and t .

For the sake of clarity we shall list Baldereschi mean value point for fcc, sc and bcc lattice as follows :

Table. (4.12)

lattice	Baldereschi point (B-Mvp)
fcc	$k_0 = \frac{2\pi}{a} (0.6223, 0.2953, 0)$
sc	$k_0 = \frac{2\pi}{a} (\frac{1}{4}, \frac{1}{4}, \frac{1}{4})$
bcc	$k_0 = \frac{2\pi}{a} (\frac{1}{6}, \frac{1}{6}, \frac{1}{2})$

The two sets of many special points for fcc lattice generated by Chadi and Cohen are listed as follows:

Table. (4.13)

C.C-set(1) : Two special points

$$k_1 = \frac{2\pi}{a} (\frac{3}{4}, \frac{1}{4}, \frac{1}{4}), \quad \alpha_1 = \frac{3}{4} ;$$

$$k_2 = \frac{2\pi}{a} (\frac{1}{4}, \frac{1}{4}, \frac{1}{4}), \quad \alpha_2 = \frac{1}{4} .$$

C.C-set(2) : Ten special points

$$k_1 = \frac{2\pi}{a} (\frac{7}{8}, \frac{3}{8}, \frac{1}{8}), \quad \alpha_1 = \frac{3}{16} ; \quad k_2 = \frac{2\pi}{a} (\frac{7}{8}, \frac{5}{8}, \frac{1}{8}), \quad \alpha_2 = \frac{1}{32} ;$$

$$k_3 = \frac{2\pi}{a} (\frac{5}{8}, \frac{5}{8}, \frac{1}{8}), \quad \alpha_3 = \frac{3}{32} ; \quad k_4 = \frac{2\pi}{a} (\frac{5}{8}, \frac{3}{8}, \frac{3}{8}), \quad \alpha_4 = \frac{3}{32} ;$$

$$k_5 = \frac{2\pi}{a} (\frac{5}{8}, \frac{3}{8}, \frac{1}{8}), \quad \alpha_5 = \frac{3}{16} ; \quad k_6 = \frac{2\pi}{a} (\frac{5}{8}, \frac{1}{8}, \frac{1}{8}), \quad \alpha_6 = \frac{3}{32} ;$$

$$k_7 = \frac{2\pi}{a} (\frac{3}{8}, \frac{3}{8}, \frac{3}{8}), \quad \alpha_7 = \frac{1}{32} ; \quad k_8 = \frac{2\pi}{a} (\frac{3}{8}, \frac{3}{8}, \frac{1}{8}), \quad \alpha_8 = \frac{3}{32} ;$$

$$k_9 = \frac{2\pi}{a} (\frac{3}{8}, \frac{1}{8}, \frac{1}{8}), \quad \alpha_9 = \frac{3}{32} ; \quad k_{10} = \frac{2\pi}{a} (\frac{1}{8}, \frac{1}{8}, \frac{1}{8}), \quad \alpha_{10} = \frac{1}{32} ;$$

(B). Evaluation Equilibrium Lattice constant by using Baldereschi point and many point scheme

We will extend our study to including the harmonic vibration in calculating the free energy at zero and finite temperatures. First we need to predict the equilibrium lattice constant for KCl crystal. It is simply to minimize the Eq.(4.12) with respect to lattice constant a . Note that assuming that KCl crystallizes in the B1 structure, the static energy u and the phonon frequency ν_i are functions of a . In order to follow the procedures described in the last subsection, we need to evaluate the free energy F in Eq.(4.12) for each assumed lattice constant.

Using Baldereschi mean value point for fcc lattice Eq.(4.12) can be approximately written as follows :

$$F = u + \frac{1}{2} \sum_{r=1}^6 h \nu_r(\vec{k}_0) + KT \sum_{r=1}^6 \ln(1 - \exp(-h \nu_r(\vec{k}_0)/KT)) \quad (4.40)$$

where \vec{k}_0 is Baldereschi point ; r sum range over the six branches of phonon modes of k_0 .

If we know a set of many special points $\{\vec{k}_i, \alpha_i; i=1, \dots, n\}$ then Eq.(4.12) becomes

$$F = u + \frac{1}{2} \sum_{r=1}^6 \sum_{i=1}^n h \nu_r(\vec{k}_i) + KT \sum_{r=1}^6 \sum_{i=1}^n \ln(1 - \exp(-h \nu_r(\vec{k}_i)/KT)) \quad (4.41)$$

Minimize Eq(4.40) or Eq(4.41) with respect to lattice constant a , we get the equilibrium lattice constant at temperature $T = 0^\circ, 300^\circ, 500^\circ, 800^\circ$ K, respectively, the results are given in table (4.14)

Table. (4.14)

Scheme	Equilibrium lattice constant (a \AA)			
	T=0 $^\circ$ K	T=300 $^\circ$ K	T=500 $^\circ$ K	T=800 $^\circ$ K
B-Mvp	6.017	6.054	6.090	6.174
C.C-set(1)	6.017	6.054	6.103	6.190
C.C-set(2)	6.017	6.054	6.096	6.182
Boyer's ⁽²⁸⁾	6.02	6.06	6.10	6.18

For comparison, the last row of the table gives the results of Boyer who showed that the summation over \vec{k} was found to be adequately converged for $N \sim 1000$, here N is the number of regularly spaced points \vec{k} in the B.Z. .

This is an example to show the efficiency of the special point scheme, of course if we need even higher degree of accuracy, we can turn to more special points for help.

(C). A Exercise : The special points for fcc and deformed fcc lattice.

As mentioned before when a fcc lattice is subjected by a uniaxial stress, it may be deformed to be a fcc or deformed fcc lattice. In order to use the many point scheme in calculating the free energy we need to generate the special points for the fcc and deformed fcc lattice.

It should be noticed that when fcc lattice is deformed to fcc or deformed fcc lattice, the lattice point group is reduced from O_h to D_{4h} or D_{2h} respectively. The "shell" of lattice vectors as well as the Eq(4.34) would be split. Moreover, the order of the "shell"s obviously depend on the ratio of π_2 to π_1 . In the most cases we are interesting in the case of $|\frac{\pi_2}{\pi_1}| < \sqrt{2}$. The different range of ratio value should be treated separately.

We report the results as follows :

1) Special points for fcc lattice

Set I three points :

$$\begin{aligned} \bar{k}_1 &= \frac{2\pi}{a} \left(\frac{1}{4\pi_1}, \frac{1}{4\pi_2}, \frac{1}{4\pi_2} \right), & \alpha_1 &= \frac{1}{4} ; \\ \bar{k}_2 &= \frac{2\pi}{a} \left(\frac{3}{4\pi_1}, \frac{1}{4\pi_2}, \frac{3}{4\pi_2} \right), & \alpha_2 &= \frac{1}{2} ; \\ \bar{k}_3 &= \frac{2\pi}{a} \left(\frac{3}{4\pi_1}, \frac{1}{4\pi_2}, \frac{1}{4\pi_2} \right), & \alpha_3 &= \frac{1}{4} ; \end{aligned} \quad (4.42)$$

Set II twenty points :

$$\begin{aligned} k_1 &= \frac{2\pi}{a} \left(\frac{3}{8\pi_1}, \frac{3}{8\pi_2}, \frac{3}{8\pi_2} \right), & k_2 &= \frac{2\pi}{a} \left(\frac{1}{8\pi_1}, \frac{1}{8\pi_2}, \frac{1}{8\pi_2} \right), \\ k_3 &= \frac{2\pi}{a} \left(\frac{3}{8\pi_1}, \frac{1}{8\pi_2}, \frac{1}{8\pi_2} \right), & k_4 &= \frac{2\pi}{a} \left(\frac{7}{8\pi_1}, \frac{1}{8\pi_2}, \frac{7}{8\pi_2} \right), \\ k_5 &= \frac{2\pi}{a} \left(\frac{1}{8\pi_1}, \frac{3}{8\pi_2}, \frac{3}{8\pi_2} \right), & k_6 &= \frac{2\pi}{a} \left(\frac{7}{8\pi_1}, \frac{3}{8\pi_2}, \frac{5}{8\pi_2} \right), \\ k_7 &= \frac{2\pi}{a} \left(\frac{7}{8\pi_1}, \frac{3}{8\pi_2}, \frac{7}{8\pi_2} \right), & k_8 &= \frac{2\pi}{a} \left(\frac{5}{8\pi_1}, \frac{1}{8\pi_2}, \frac{7}{8\pi_2} \right), \\ k_9 &= \frac{2\pi}{a} \left(\frac{7}{8\pi_1}, \frac{1}{8\pi_2}, \frac{5}{8\pi_2} \right), & k_{10} &= \frac{2\pi}{a} \left(\frac{5}{8\pi_1}, \frac{1}{8\pi_2}, \frac{1}{8\pi_2} \right), \end{aligned}$$

$$\begin{aligned}
\vec{k}_{11} &= \frac{2\pi}{a} \left(\frac{5}{8\pi_1}, \frac{3}{8\pi_2}, \frac{5}{8\pi_2} \right), & \vec{k}_{12} &= \frac{2\pi}{a} \left(\frac{7}{8\pi_1}, \frac{1}{8\pi_2}, \frac{1}{8\pi_2} \right), \\
\vec{k}_{13} &= \frac{2\pi}{a} \left(\frac{5}{8\pi_1}, \frac{3}{8\pi_2}, \frac{7}{8\pi_2} \right), & \vec{k}_{14} &= \frac{2\pi}{a} \left(\frac{5}{8\pi_1}, \frac{1}{8\pi_2}, \frac{5}{8\pi_2} \right), \\
\vec{k}_{15} &= \frac{2\pi}{a} \left(\frac{7}{8\pi_1}, \frac{3}{8\pi_2}, \frac{3}{8\pi_2} \right), & \vec{k}_{16} &= \frac{2\pi}{a} \left(\frac{5}{8\pi_1}, \frac{3}{8\pi_2}, \frac{3}{8\pi_2} \right), \\
\vec{k}_{17} &= \frac{2\pi}{a} \left(\frac{7}{8\pi_1}, \frac{1}{8\pi_2}, \frac{3}{8\pi_2} \right), & \vec{k}_{18} &= \frac{2\pi}{a} \left(\frac{1}{8\pi_1}, \frac{1}{8\pi_2}, \frac{3}{8\pi_2} \right), \\
\vec{k}_{19} &= \frac{2\pi}{a} \left(\frac{5}{8\pi_1}, \frac{3}{8\pi_2}, \frac{1}{8\pi_2} \right), & \vec{k}_{20} &= \frac{2\pi}{a} \left(\frac{3}{8\pi_1}, \frac{1}{8\pi_2}, \frac{3}{8\pi_2} \right).
\end{aligned} \tag{4.43}$$

with the weighting factors $\alpha_i = 1/24$, $i=1,2,\dots,16$; and $\alpha_j = 1/12$, $j=17,18,19$ and 20 .

ii) Special points for deformed fct lattice :

Set III two points:

$$\vec{k}_1 = \frac{2\pi}{a} \left(\frac{1}{4\pi_1}, \frac{h}{4\pi_2}, \frac{h}{4\pi_2} \right); \quad \alpha_1 = \frac{1}{2}; \tag{4.44}$$

$$\vec{k}_2 = \frac{2\pi}{a} \left(\frac{3}{4\pi_1}, \frac{h}{4\pi_2}, \frac{h}{4\pi_2} \right); \quad \alpha_2 = \frac{1}{2}.$$

where

$$h = (\sqrt{2} \cos \frac{1}{2} \varphi)^{-1} \tag{4.45}$$

Set IV Eight points :

$$\begin{aligned}
\vec{k}_1 &= \frac{2\pi}{a} \left(\frac{3}{8\pi_1}, \frac{3h}{8\pi_2}, \frac{3h}{8\pi_2} \right), & \vec{k}' &= \frac{2\pi}{a} \left(\frac{1}{8\pi_1}, \frac{h}{8\pi_2}, \frac{h}{8\pi_2} \right), \\
\vec{k}_3 &= \frac{2\pi}{a} \left(\frac{3}{8\pi_1}, \frac{h}{8\pi_2}, \frac{h}{8\pi_2} \right), & \vec{k}_4 &= \frac{2\pi}{a} \left(\frac{1}{8\pi_1}, \frac{3h}{8\pi_2}, \frac{3h}{8\pi_2} \right), \\
\vec{k}_5 &= \frac{2\pi}{a} \left(\frac{7}{8\pi_1}, \frac{3h}{8\pi_2}, \frac{3h}{8\pi_2} \right), & \vec{k}_6 &= \frac{2\pi}{a} \left(\frac{7}{8\pi_1}, \frac{h}{8\pi_2}, \frac{h}{8\pi_2} \right), \\
\vec{k}_7 &= \frac{2\pi}{a} \left(\frac{5}{8\pi_1}, \frac{3h}{8\pi_2}, \frac{3h}{8\pi_2} \right), & \vec{k} &= \frac{2\pi}{a} \left(\frac{5}{8\pi_1}, \frac{h}{8\pi_2}, \frac{h}{8\pi_2} \right).
\end{aligned} \tag{4.46}$$

with equal weighting factor $\alpha_i = 1/8$, $i=1,2,\dots,8$; and the h is given by Eq(4.45).

The validity of these sets of the special points should be proved in practice.

Concluding Remarks

1) In conclusion we emphasise that our static results are incomplete and in the nature of a preliminary survey to indicate the role of a uniaxial stress in addition to a hydrostatic pressure plays in the transformation. This study will be extended to include the harmonic vibrations at zero and finite temperature. It would tell us the effects of temperature on the transformation. By using the procedure described in the section IV and incorporating the many point scheme in evaluation the B.Z. sums, this in principle can be done. The problem is that, on one hand to predict correct configuration needs very high accuracy in calculating Gibbs free energy; on the other hand using more special points requires more computational work. So a compromise should be made to ensure a sufficient accuracy.

2) As mentioned, a detailed experimental description on B1 to B2 transformation in RbI has been presented. It is instructive to give a similar theoretical calculation for RbI. The results will then be compared with the experimental facts.

3) It was shown that a static calculation usually gives a satisfactory result for a system at equilibrium or near equilibrium conditions: While as the system evolves its configurations to reach a instable point, the theoretical argumentation will not be mathematically consistent. Now we can turn to new MD method for help. This new MD method provides a powerful tool for the investigation of polymorphic transitions. In this method once the model is given, the results can be obtained in an exact theoretically consistent way for any reasonable thermodynamic conditions. We will use this new MD method to study the uniaxial stress (in addition to hydrostatic pressure) induced B1 to B2 transformation in KCl. In order to keep on our calculation as a parameter free one, at first the parameterized Gordon-Kim potential will be used.

4) Using the new MD method to investigate the roles played by point defects in the transformation. It is possible that these defects in the crystal may induce local stresses that trigger the transformation inhomogeneously.

Acknowledgments

I would like to express my sincere thanks to my supervisor Prof. M. Parrinello for introducing me to this very interesting field, for his earnest and tireless instructions, and for his invaluable encouragement during the course of the work. I wish to thank the following Professors: A. Baldereschi, G. C. Ghirardi, P. Giaquinta, N. Majlis, A. Nobile, M. Parrinello, R. Resta, A. Stella, F. Toigo, E. Tosatti, M. Tosi, and C. Verzegnassi. I have benefited greatly from their lectures. Prof. R. Resta is acknowledged for his several enlightening discussions on lattice dynamics. Heartfelt thanks are due to Prof. A. Nobile for a lot of helpful advices on computer programming. I am grateful to Prof. P. Budinich, L. Fonda and the International School for Advanced Studies in Trieste for a fellowship and for their hospitality. The SISSA staff and the ICTP library are gratefully acknowledged for their helpful services.

References

- (1) E. Madelung, Phys. Z. 11, 898, (1910)
- (2) M. Born and J. E. Mayer, Z. Phys. 75, 1 (1932)
- (3) M. Born, Dynamik der Kristallgitter (teubner, Leipzig, 1915)
- (4) A. Hylleraus, Z. Phys. 63, 771 (1930)
- (5) R. Landshoff, Z. Phys. 102, 120, (1936)
- (6) J. Yamashita, J. Phys. Soc. Jap, 7, 284 (1952)
- (7) S. O. Lundqvist, Ark. Fys, 8, 177 (1954)
- (8) M. P. Tosi, in "Solid St. Phys." 16, 1, (1964), and references therein
- (9) P. O. Lowdin, Adv. Phys. 5, 1 (1966)
- (10) A. N. Basu and S. Sengupta, Phys. Rev, B, 14, 2633 (1976)
- (11) Jai. Shanker, V. C. Jain and J. P. Singh Phys Rev B, 22, 1083 (1980)
- (12) H. D. Merchant, K. K. Srivastava, H. D. Pandey, CRC Critical Rev in Sol. St. Science, 451 (1973)
- (13) W. A. Bassett, T. Takahashi and J. K. Campbell, Trans. Am. Crystallogr. Assoc, 5, 93 (1969) and references therein.
- (14) J. C. Slater, Phys rev, 27, 488 (1924)
- (15) A. Lacam and J. Peyronneau, Rev. Phys. Appl, 10, 293 (1975)
- (16) P. W. Bridgman in "Phys. of High Pressure " Chap. v111, G. Bell. London (1949)
- (17) G. Wagner and Z. Lippert, Z. Phys. Chem, B21, 471 (1933); Z. Phys. Chem, B71, 263 (1936)
- (18) C. E. Weir and G. J. Piermarini, J. Res. nat. Bar. Stand 68a, 105, (1964)
- (19) V. V. Evdokimova and L. F. Vereshchagin, Soviet Phys. J. E. T. P, 16, 895, (1963)
- (20) O. Blaschko. et. al. Phys. Rev B, 20, 1157 (1979)
- (21) R. B. Jacobs. Phys. rev. 54, 468 (1938)
- (22) M. Born and K. Huang "Dynamical Theory of Crystal Lattice " (Oxford 1954)
- (23) M. P. Tosi and T. Arai, in "Advances in High Pressure Research" Ed. by R. S. Bradicy. Vol 1 (1966)
- (24) M. P. Tosi and F. G. Fumi, Int. J. Phys. Chem. Sol, 23, 359, (1962)
- (25) Y. S. Kim and R. G. Gordon, Phys. Rev B9, 3548 (1974)
- (26) A. J. Cohen and R. G. Gordon, Phys. Rev B12, 3228 (1975); Y. S. Kim and R. G. Gordon. J. Chem. Phys, 60, 4332 (1974)
- (27) R. G. Gordon and Y. S. kim. J. Chem. Phys 56, 3122 (1972)

- (28) L.L. Boyer. Phys Rev B23, 3673 (1981)
- (29) H. Shoji, Z. Kristallogr, Kristallgeorn, Kristallchem, 77, 381, (1973)
- (30) M.J. Buerger, in "Phase Transformation in Solids" Edited by R. Smoluchowski, J.E. Mayer and W.A. Weyl (Wiley, New York, 1951)
- (31) W.L. Fraser and S.W. Kennedy, Acta Crystallogr. Soc A30, 13 (1951)
- (32) M. Watanabe, M. Tokonami and N. Imoto, Acta Crystallogr Sec A 33, 294 (1977)
- (33) O. Bloeschko et al. J. Phys (Paris) 38, 407, (1977)
- (34) O. Bloeschko et al. Rev. Sci. Instrum. 45, 256 (1974)
- (35) O. Bloeschko et al. Phys. Rev. B11, 3960 (1975)
- (36) O. Bloeschko et al. Phys. Rev B23, 3017 (1981)
- (37) M. Parrinello and A. Rahman, Phys Rev. Letter. 45, 1196 (1980)
- (38) M. Parrinello and A. Rahman, J. De. Phys C6, 511 (1981)
- (39) M. Parrinello and A. Rahman. JAppl. Phys 52, 7182 (1981)
- (40) M. Parrinello and A. Rahman, J. Chem. Phys 76, 2662 (1982)
- (41) F. Mlstein and B. Farber. Phys Rev Lett. 44, 277 (1980)
- (42) N.C. Banik et al. Phys. Rev Lett. 43, 456 (1979)
- (43) J.Y. Buzare et al. Phys Rev. Lett. 42, 465 (1979)
- (44) C. Kittel. "Introduction to Solid State Phys" (5th edition), John Wiley Inc, 1976
- (45) N.W. Ashcroft and N.D. Mermin, "Solid State Phys", Holt Rinehart, Ninston, (1976)
- (46) L.P. Bonckaerdt, R. Smoluchowski and E. Wigner, Phys Rev, 50, 58 (1936)
- (47) W.B. Daniels and C.S. Smith. in "The Phys and Chem of High Pressures" P.50, Society of Chemical Industry, London (1963)
- (48) J.R. Hardy and A.M. Karo, in "Lattice Dynamics " Ed. by R.F. wall, P195, Pergaman Press, London
- (49) J.W. Kenary, A.R. Ubbelohde and A. Woodward, Proc Roy Soc A, 208, 158 (1971)
- (50) S. Chatierji and A.L. Mackay and J.W. Jeffery. J. Appl. Cryst. 4, 175 (1971)
- (51) J.P. mansen and I.R. McDonald, in "Theory of Simple Liquids" Chap 3, Academic Press, London, New York, San Fracisco (1976)
- (52) A. Rahman, in "Correlation Function and Quasiparticle Interactions in Condensed Matter " (Ed. J. Woods Halley, Plenum, 1977)
- (53) B.J. Alder and T.E. Wainwright, J. Chem. Phys. 27, 1208 (1957)
- (54) B.J. Alder and T.E. Wainwright. J. Chem. Phys. 31, 459 (1959)

- (55) A. Rahman, Phys Rev, 136A, 405 (1964)
- (56) A. Rahman, J. Chem Phys, 45, 258 (1966)
- (57) L. Verlet, Phys Rev, 159, 98 (1967)
- (58) L. Verlet, Phys Rev, 163, 201 (1968)
- (59) D. Levesque and L. Verlet, Phys Rev A2, 2514 (1970)
- (60) D. Levesque et al. Phys Rev A7, 1690 (1973)
- (61) M. J. L. Sangster and M. Dixon, Adv. in Phys, 25, 247 (1976) and references therein.
- (62) M. Parrinello, A. Rahman and P. Vashishta, to be published.
- (63) A. Rahman and P. Vashishta, in "Molecular Dynamics Studys of Superionic conductors ", Argonne National Laboratory, Argonne, Illionois (1981)
- (64) a). C.W. Gear, ANL Report 7126, Argonne National Laboratory, (1966).
- b). C.W. Gear, "Numerical Initial Value Problem in Ordinary Differential Equations " (Preitice Hall, Englewood Cliffs N. J, 1971)
- (65) H. C. Andersen, J Chem. Phys. 72, 2384 (1980)
- (66) L. D. Landau and E. M. Lifshiz, Theory of Elasticity, (Pergaman, Oxford, 1955)
- (67) A critical examination of Gordon-Kim potential can be found in M. J. Clungston, Adv. in. Phys. 27, 893 (1978).
- (68) P. P. Ewald. Ann. Physik (4) 64, 257 (1921)
- (69) C. Kittel, " A Introduction to Solid State Phys. ", Appendix A, 2nd edition, Wiley, Inc (1956)
- (70) A. A. Maradudin, E. W. Montroll, and G. H. Weiss, In "Theory of Lattice Dynamics in the Harmonic Approximation" edited by F. Seitz and D. Turnbull (Academic NEW York)
- (71) J. R. Hardy. Phil. Mag, 7, 715 (1962).
- (72) G. F. Koster, In "Solid State Phys." 5, 177, (1957)
- (73) A. Baldereschi, Phys. Rev. B7, 5212 (1973)
- (74) A. Baldereschi, Bull. Am. Phys. Soc, 17, 237 (1972)
- (75) D. J. Chadi and M. L. Cohen, Phys. Rev B8, 5747 (1973).
- (76) H. J. Monkhorst and J. D. Pack, Phys. Rev B13, 5188 (1975).
- (77) V. K. Bashenov and M. Bardashova and A. M. Matul, Phys. Stat. Sol. (b) 80 K89 (1977)
- (78) P. J. Lin-Chung, Phys Stat Sol (b), 85, 743 (1978).